Andrzej PAZUR
Air Force Institute of Technology
e-mail: andrzej.pazur@itwl.pl; ORCID: 0000-0002-3126-1110

Mirosław WITOŚ
Air Force Institute of Technology
e-mail: miroslaw.witos@itwl.pl; ORCID: 0000-0002-9660-4399

Andrzej SZELMANOWSKI
Air Force Institute of Technology
e-mail: andrzej.szelmanowski@itwl.pl; ORCID: 0000-0001-6183-0241

Jerzy BOROWSKI
Air Force Institute of Technology
e-mail: jerzy.borowski@itwl.pl

Wojciech WRÓBLEWSKI
Polish Air Force University
e-mail: w.wroblewski@law.mil.pl

DOI: 10.55676/asi.v4i2.94

MEASURE AND ANALYSIS OF 3D MAGNETIC DEVIATION IN AERONAUTICAL MAGNETIC HEADING SYSTEMS AND HELMET MOUNTED CUEING SYSTEM

POMIAR I ANALIZA ODCHYLENIA MAGNETYCZNEGO 3D W LOTNICZYCH MAGNETYCZNYCH SYSTEMACH NAPROWADZANIA I SYSTEMACH NAPROWADZANIA MONTOWANYCH NA HEŁMIE LOTNICZYM

Abstract

In the XXI century, magnetic sensors and measurements are widely used in many diverse applications. The aspects of magnetic measurements and deviation in the Magnetic Heading System (MHS) and the Helmet Mounted Cueing System (HMCS) onboard civilian and military aircraft have been presented. In the beginning, the magnetometers market and application area, and the corresponding sensor measuring ranges and errors are presented. Next, the considerations focused on the theory of magnetic deviation considering the influence of soft and hard iron and the magnetic field generated by electrical devices. The mathematical relationships describing the components of the magnetic deviation and measurement path were given. Then, an innovative element is a simulation model, developed in the Matlab-Simulink package, enabling the determination of 2D horizontal deviation and 3D spatial deviation for the given spatial orientation angles. Finally, the selected results of the research are presented.

Streszczenie

W XXI wieku czujniki i pomiary magnetyczne są szeroko stosowane w wielu różnych aplikacjach. W artykule przedstawiono aspekty pomiarów magnetycznych i odchyleń w Magnetic Heading System (MHS) i Helmet Mounted Cueing System (HMCS) na pokładzie samolotów cywilnych i wojskowych. Na początku omówiono rynek magnetometrów i obszar ich zastosowań oraz odpowiadające im zakresy pomiarowe i błędy czujników. Następnie rozważania skupiły się na teorii dewiacji magnetycznej z uwzględnieniem wpływu miękkiego i twardego żelaza oraz pola magnetycznego generowanego przez urządzenia elektryczne. Podano zależności matematyczne opisujące składowe odchylenia magnetycznego oraz ścieżkę pomiarową. Następnie nowatorskim elementem jest model symulacyjny, opracowany w pakiecie Matlab-Simulink, umożliwiający wyznaczenie dewiacji poziomej 2D oraz dewiacji przestrzennej 3D dla zadanych kątów orientacji przestrzennej. Na koniec przedstawiono wybrane wyniki badań. Pokazano przykładowe wyniki

Artykuł wpłynął do redakcji: 16.10.2023 / Zatwierdzono do publikacji: 30.12.2023

The exemplary results of the analysis of magnetic deviation occurring on military airplanes are shown. The purposefulness of using harmonic analysis to improve the accuracy of deviation compensation, especially in HMCS applications, was indicated. The purposefulness of 3D deviation analysis has been demonstrated. Based on the conducted research, the developed 3D deviation model and the residual deviation properties measured in the vicinity of the aircraft were verified. The need to provide a 3D deviation model based on experimental data was indicated. Experimental data made it possible to determine the azimuth of the occurrence of the greatest deviation value during ground surveys of the aircraft population.

Keywords: aviation, 3D magnetic deviation, magnetometer, tracking system, Helmhelmet-Mounted Cueing System

analizy dewiacji magnetycznej występującej na samolotach wojskowych. Wskazano na celowość wykorzystania analizy harmonicznej do poprawy dokładności kompensacji dewiacji, szczególnie w zastosowaniach HMCS. Wykazano celowość analizy dewiacji 3D. W oparciu o przeprowadzone badania zweryfikowano opracowany model odchylenia 3D oraz właściwości odchylenia resztkowego zmierzone w pobliżu samolotu. Wskazano na potrzebę opracowania modelu dewiacji 3D w oparciu o dane eksperymentalne. Dane eksperymentalne pozwoliły na wyznaczenie azymutu występowania największej wartości odchylenia podczas badań naziemnych populacji statków powietrznych.

Słowa kluczowe: lotnictwo, odchylenie magnetyczne 3D, magnetometr, system naprowadzania, hełm lotniczy

1. INTRODUCTION

Magnetic field measurements are widely used in many different fields of technology and supported by modern measurement techniques and computer simulations[1]. However, the magnetic field sensor[2] is still the basic element that determines the accuracy of the measurement.

The market for magnetic field sensors (vector and scalar) is the fastest growing among all various sensors. The global magnetic sensor market was valued at USD 2376.48 million in 2020, and registering a compound annual growth rate (CAGR) of 6.51% over the forecast period 2021 – 2026[3]. Today, magnetic and electromagnetic

[1] COMSOL Multiphysics® Modeling Software, http://www.comsol.com; FEMM Finite Element Method Magnetics, https://www.femm.info/wiki/HomePage; OPERA Electromagnetic And Electromechanical Simulation, https://www.3ds.com/products-services/simulia/products/opera/; EMWORKS Electromagnetic Simulation Software with Built-in Thermal, Motion and Structural Analyses, https://www.emworks.com; Notaroš B.M., MATLAB-Based Electromagnetics, Pearson, 2014, 416 pp., https://www.pearson.com/us/higher-education/program/Notaros-MATLAB-Based-Electromagnetics/PGM2486281.html?tab=resources.

[2] https://www.aichi-steel.co.jp/ENGLISH/smart/mi/products/; https://www.bartington.com/high-precision-magnetometers/; https://www.bosch-sensortec.com/products/motion-sensors/; https://www.gemsys.ca; https://www.geometrics.com; https://aerospace.honeywell.com; http://micromagnetics.com; http://www.dowaytech.com/en/; https://www.pnicorp.com; https://www.sensixs.nl.

[3] Magnetic Sensors Market - Growth, Trends, Covid-19 Impact, And Forecasts (2021 - 2026), https://mordorintelligence.com/industry-reports/magnetic-sensor-market.

 DOI: 10.55676/asi.v4i2.94

measurements are widely used in different applications[4], e.g. informatics devices (data carriers, smartphones, tablets), processes monitoring systems in cars, metrology (current intensity measurements, encoders), geology, archeology, medicine, aerial and marine reconnaissance and non-destructive testing, Figure 1. A wide range of magnetometers are now on the market, their prices (from single to thousands of U.S. dollars depending on the type, accuracy and measuring range) are decreasing from year to year and metrological parameters are improving. Moreover, new magnetometer applications, designs and developments are coming to light continuously[5].

There are many different types of magnetometers designed for different applications. For very small magnetic fields (fT level), we can find SQIUD sensors[6] and nitrogen-vacancy (NV) diamond sensor[7]; for small magnetic fields (pT level) - atomic scalar magnetometers[8], magnetoimpedance sensors (MI)[9], tunneling magnetoresistance

[4] Bennett J.S., Vyhnalek B.E., Greenall H., Bridge E.M., Gotardo F., Forstner S., Harris G.I., Miranda F.A., Bowen W.P., Precision Magnetometers for Aerospace Applications: A Review. Sensors 2021, 21, 5568, DOI: 10.3390/s21165568; Oravec M., Lipovský P., Šmelko M., Adamčík P., Witoś M., Low-Frequency Magnetic Fields in Diagnostics of Low-Speed Electrical and Mechanical Systems. Sustainability 2021, 13, 9197, DOI: 10.3390/su13169197; Carletta S., Teofilatto P., Farissi M.S., A Magnetometer-Only Attitude Determination Strategy for Small Satellites: Design of the Algorithm and Hardware-in-the--Loop Testing. Aerospace 2020, 7, 3, DOI: 10.3390/aerospace7010003; Liu H., Dong H., Ge J., Liu Z., An Overview of Technologies for Geophysical Vector Magnetic Survey: A Case Study of the Instrumentation and Future Directions. arXiv 2020, arXiv:2007.05198; Korth H., Strohbehn K., Tejada F., Andreou A.G., Kitching J., Knappe S., Lehtonen S.J., London S.M., Kafel M., Minia-ture atomic scalar magnetometer for space based on the rubidium isotope 87Rb, J. Geophys. Res. Space Physics, 2016, 121, DOI:10.1002/ 2016JA022389; Singh S.P., Magnetoencephalography: Basic principles. Ann Indian Acad Neurol. 2014;17(Suppl 1):S107-S112. DOI: 10.4103/0972-2327.128676; Johnston M.J.S., Review of magnetic and electric field effects near active faults and volcanoes in the U.S.A., Physics of the Earth and Planetary Interiors, 1989, Vol 57, Issue 1-2, 47-63, DOI: 10.1016/0031-9201(89)90213-6; Haoui A., Kavaler R., Varaiya P., Wireless magnetic sensors for traffic surveillance, Transportation Research Part C: Emerging Technologies, 2008, Vol. 16, Issue 3, 294-306, DOI: 10.1016/j.trc.2007.10.004.

[5] Magnetic Field Sensors, https://www.analog.com/en/parametricsearch/11290#/; Inertial Measurement Units (IMU), https://www.analog.com/en/parametricsearch/11172#/; XEN1210 Magnetic Sensor, datasheet, www.sensixs.nl; Ellipse2-A: Miniature AHRS, https://www.navigationsolutions.eu/product/ellipse2-miniature-ahrs/; https://www.xsens.com/products/.

[6] SQUID Sensors: Fundamentals, Fabrication and Applications, ed. H. Weinstock,NATO ASI Series, Kluwer Academic Pub-lishers 1996, DOI: 10.1007/978-94-011-5674-5; http:// http://www.magnicon.com/fileadmin/download/datasheets/Magnicon_Squids.pdf.

[7] Schloss J.M., Barry J.F., Turner M.J., Walsworth R.L., Simultaneous Broadband Vector Magnetometry Using Solid-State Spins, Phys. Rev. Applied 2018, 10, 034044, https://journals.aps.org/prapplied/abstract/10.1103/PhysRevApplied.10.034044; Fescenko I., Jarmola A., Savukov I., Kehayias P., Smits J., Damron J., Ristoff N., Mosavian N., Acosta V.M., Diamond magnetometer enhanced by ferrite flux concentrators, Physical Review Research 2020, 2, 023394, DOI: 10.1103/PhysRevResearch.2.023394.

[8] https://www.bartington.com/high-precision-magnetometers/; https://www.gemsys.ca; Korth H., Strohbehn K., Tejada F., Andreou A.G., Kitching J., Knappe S., Lehtonen S.J., London S.M., Kafel M., Minia-ture atomic scalar magnetometer for space based on the rubidium isotope 87Rb, J. Geophys. Res. Space Physics, 2016, 121, 7870–7880, DOI: 10.1002/2016JA022389; Hoekstra B., Mhaskar R., MFAM: Miniature Fabricated Atomic Magnetometer for Autonomous Magnetic Surveys, Drones Applied to Geophysical Mapping Workshop SEG 2017, https://seg.org/Portals/0/SEG/News%20and%20Resources/Near%20Surface/Resources/Drones_Workshop/6_MFAM-Miniature%20Atomic%20Magnetometer%20for%20Autonomous%20Magnetic%20Surveys_Hoekstra.pdf.

[9] https://www.aichi-steel.co.jp/ENGLISH/smart/mi/products/.

(TMR)[10] and flux-gate sensors[11]; for medium fields (nT and μT level) – magnetoresistance sensors (MR) and Giant Magnetoresistance (GMR)[12]; for high magnetic field (from μT to kT level) - Hall and Q-Hall sensors[13], Figure 2.

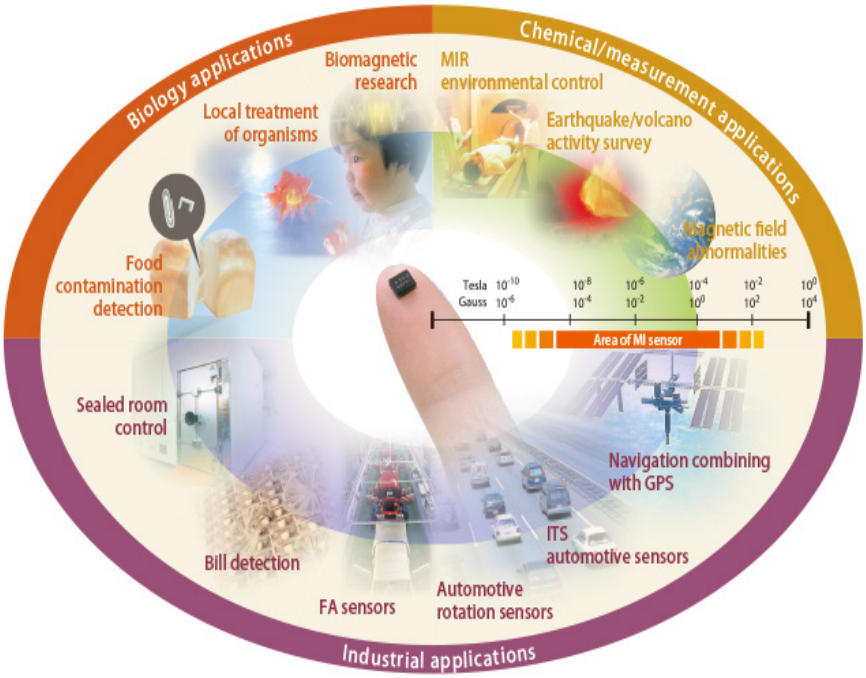

Figure 1. The varied magnetometer applications

Source: Mohri K., Uchiyama T., Shen L.P., Cai C.M. , Panina L.V., Amorphous Wire and CMOS IC-Based Sensitive Mi-cro-Magnetic Sensors (MI Sensor and SI Sensor) for Intelligent Measurements and Controls, Journal of Magnetism and Magnetic Materials, 2002, Vol. 249, No. 1-2, pp. 351-356, DOI: 10.1016/S0304-8853(02)00558-9.

10 http://micromagnetics.com; http://www.dowaytech.com/en/.

11 Korepanov V., Marusenkov A., Flux-Gate Magnetometers Design Peculiarities. Surv Geophys 2012, 33, 1059–1079, DOI: 10.1007/s10712-012-9197-8; Bartington Fluxgate Magnetometer, 3-Axis, Low Noise, https://gmw.com/product/mag-03-mag-13/; DRV425 Fluxgate Magnetic-Field Sensor, datasheet, Texas Instrument, SBOS729A –October 2015–Revised March 2016.

12 https://www.nve.com/webstore/catalog/index.php?view=all&cPath=27.

13 Hall Effect Sensing And Application, Honeywell, https://sensing.honeywell.com/hallbook.pdf.

 DOI: 10.55676/asi.v4i2.94

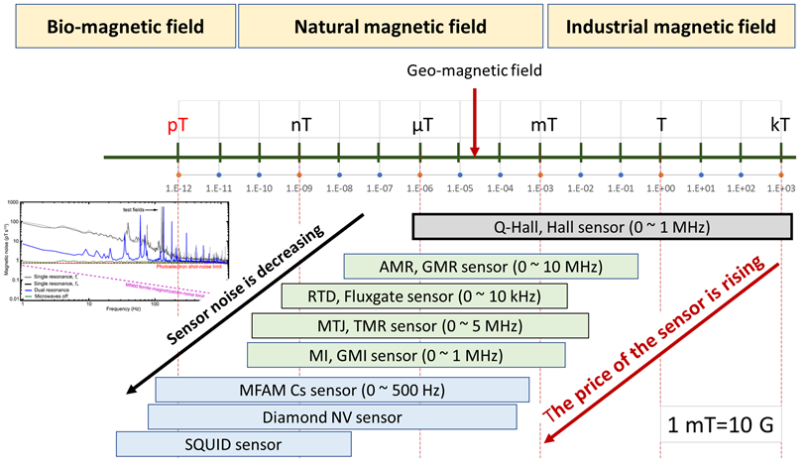

Figure 2. Basic magnetometer parameters and areas of application (measurement range, price and sensor noise)

Source: own elaboration.

To illustrate the values of possible measurement errors with the use of magnetometers, selected parameters of the above sensors are presented below, Table 1. Some parameters of the sensors in the catalog data are unknown, hence the need to designate and calibrate measurement path in order to obtain the required accuracy[14]. The sensors are calibrated and validate in a reference magnetic field using:

- 3D Helmholtz coil and function generator[15] – very precise calibration result obtained only in laboratory conditions;
- reference magnetometer, static data on the position of the sensor in the geographic coordinate system (laboratory or airport) and numerical model of main part of Earth's field IGRF-13[16] or WMM[17] – calibration result includes errors of omitted components of the Earth's mantle and crust (higher harmonics of the field with wavelength < 2600 km) and the cosmic component that intensifies during magnetic

14 ISO 5725-1:1994 Accuracy (trueness and precision) of measurement methods and results – Part 1: General principles and definitions; ISO 5725-6:1994 Accuracy (trueness and precision) of measurement methods and results – Part 6: Use in practice of accuracy values; Accuracy classes of measuring instruments, International Recommendation OIMLR34, edition 1979 (E), International Or-ganization of Legal Metrology, https://www.oiml.org/en/files/pdf_r/r034-e79.pdf.

15 Lassahn M.P., Trenkler G., Vectorial calibration of 3D magnetic field sensor arrays, in IEEE Transactions on Instrumen-tation and Measurement, vol. 44, no. 2, pp. 360-362, April 1995, DOI: 10.1109/19.377852; PalmGauss™ S (PGSC-5G), https://www.aichi-steel.co.jp/ENGLISH/smart/mi/products/palm-gauss.html.

16 Alken P., Thébault E., Beggan C.D. et al., International Geomagnetic Reference Field: the thirteenth generation. Earth Planets Space 2021, 73, 49, DOI: 10.1186/s40623-020-01288-x; International Geomagnetic Reference Field, https://www.ngdc.noaa.gov/IAGA/vmod/igrf.html.

17 Chulliat A., Brown W., Alken P., Beggan C., Nair M., Cox G., Woods A., Macmillan S., Meyer B., Paniccia M., The US/UK World Magnetic Model for 2020-2025: Technical Report, National Centers for Environmental Information, NOAA, 2020. DOI: 10.25923/ytk1-yx35; The World Magnetic Model and Associated Software, https://www.ngdc.noaa.gov/geomag/WMM/soft.shtml.

storms[18]. These data are available in the high precision measurement data of the INTERMAGNET network observatories[19] located near our sensor and the Enhanced Magnetic Model (EMM) which extends to degree and order 790, resolving magnetic anomalies down to 51 km wavelength[20] or model of the Earth's Crustal Field EMAG2 with 2-arc-minute spatial resolution[21];

– dynamic data from Satellite Positioning Systems (GPS, GLONASS, Galileo, BeiDuo, QZSS, IRNSS-NAVIC) or / and an inertial navigation system (INS) or Attitude and Heading Reference System (AHRS) or / and ground-based radio navigation system (LORAN, TACAN, NDB, VOR/DME, ILS) when the object and sensor are moving - the result of compass calibration contains errors resulting from the dynamics and trajectory of the object's movement, including linear accelerations, pitch and roll angles and course[22].

Table 1. Selected parameters of the digital magnetic sensors

Parameter	Unit	ADIS 16405	AMI 305	RM 3100	FXOS 8700	XEN1210
Type	---	3D AMR	3D MI	3D MI	3D TMR	1D Q-Hall
Dynamic range	μT	±350	±1 200	±800	±1200	±63000
channel resolution	nT/LSB	50	600	13, 26 or 50	100	7.5
Sensivity temperature coefficient (lσ)	ppm/K	600	*No data*	0	100	400
Axis non-orthogonality	degrees	0.25	≤0.6	*PCB*	*No data*	*PCB*
Axis misalignment	Degrees	0.5	*No data*	*PCB*	*No data*	*PCB*
Bias temperature coefficient	nT/K	50	±30	0	800	15
Nonlinearity	% of FS	0.5	0.5	0.5 (for ±200μT)	0.5	*No data*
Initial bias error	nT	±400	*No data*	*No data*	±10000	±1500
Hysteresis	nT	*No data*	*No data*	15	0.5% FS	10
Output noise and Noise density (no filtering)	nT rms $nT/\sqrt{Hz}$	125 6.6	*No data* *No data*	30, 20 or 15 1.2	≤1.5 μT 100 (at 100 Hz band	290 - 5800 55
3 dB band	Hz	1540	*No data*	*No data*	100	*No data*
Max. sample rate	Hz	1200	1000	1600	800	4882

Source: ADIS16405 Triaxial Inertial Sensor with Magnetometer, https://www.analog.com/media/en/technical-documentation/data-sheets/ADIS16405.pdf; AMI305 Electronic Compass, ttps://aichi-mi-test.jimdo.com/e-home-new/electronic-compass/ami305-3-axis-compass/; RM3100 Geomagnetic Sensor, https://www.pnicorp.com/rm3100/; FXOS8700CQ 6-axis sensor with integrated linear accelerometer and magnetometer, Rev. 8 – 25 April 2017, https://www.nxp.com/docs/en/data-sheet/FXOS8700CQ.pdf; XEN1210 Magnetic Sensor, https://www.sensixs.nl/data/documents/XEN1210.pdf.

18 Space Weather Prediction Center National Oceanic And Atmospheric Administration, https://www.swpc.noaa.gov/.

19 http://www.intermagnet.org; https://intermagnet.github.io/.

20 Enhanced Magnetic Model (EMM), https://www.ngdc.noaa.gov/geomag/EMM/.

21 EMAG2: Earth Magnetic Anomaly Grid (2-arc-minute resolution), http://geomag.colorado.edu/emag-2-earth-magnetic-anomaly-grid-2-arc-minute-resolution.html; EMAG2: Earth Magnetic Anomaly Grid (2-arc-minute resolution), https://www.ngdc.noaa.gov/geomag/emag2_download.html.

22 FAA-H-8083-15B Instrument Flying Handbook, U.S. Department of Transportation, Federal Aviation Administration, Flight Standards Service, Oklahoma 2012.

 DOI: 10.55676/asi.v4i2.94

The development of models of the Earth's magnetic field and digital magnetometers cooperating with processors brings the moment when magnetic anomalies of the Earth's mantle and crust will be used for precise navigation, just like animals[23].

Magnetic navigation (a passive navigation system) is still the most immune to external interference, unlike:

- satellite systems exposed to jammed from the enemy action;
- INS and AHRS systems sensitive to power outages of the on-board network;
- radio navigation systems sensitive to power outages of the on-board network or the destruction of radio finders by enemy action.

The classic compass fulfills its function even during a power failure therefore, aviation and naval transport regulations require the compass to be fully functional, including knowledge of the magnetic deviation contributed by local sources of the magnetic field.

The compass calibration requirements for small aircraft (less than 12.500 lbs maximum take-off weight) can be found in FAR's 23.1327 and 23.1547. For large aircraft (more than 12.500 lbs maximum take-off weight), the compass calibration requirements can be found in FAR's 25.1327 and 25.1547. FAR's 27 and 29 have the same requirements for small and large helicopters. The magnetic direction indicator (compass) is a required instrument under 14 CFR part 91 for Visual Flight Rules (VFR)/ Instrument Flight Rules (IFR) operations[24]. According to the SOLAS chapter V 'Safety of navigation' approved alternatives are permitted for: Standard magnetic compass, Pelorus or compass bearing device and Correction to heading/bearing e.g. e-compasses but only on small cargo ships of less than 150 GT no spare magnetic compass is required[25].

Vector magnetometers are also used in helmet systems[26]. A good helmet system ensures achievement of advantage in combat improves the general performance of the aircraft, increases the chances of completing the mission and ensures the survival of the crew. The helmet mounted cueing system is a key element of the weapon control

[23] Phillips J.B., Magnetic Navigation, Journal of Theoretical Biology, 1996, Volume 180, Issue 4, pp. 309-319, DOI: 10.1006/jtbi.1996.0105; Canciani A., Magnetic Navigation, https://www.gps.gov/governance/advisory/meetings/2018-12/canciani.pdf.

[24] AC 43-215 - Standardized Procedures for Performing Aircraft Magnetic Compass Calibration Document Information, FAA 2017, https://www.faa.gov/regulations_policies/advisory_circulars/index.cfm/go/document.information/documentID/1031648.

[25] Solas Shipborne Navigational Carriage Requirements, https://www.radioholland.com/about-radio-holland/regulations/navigational-carriage-requirements/#150GT; 382(X) Magnetic compasses carriage and performance standards, https://puc.overheid.nl/nsi/doc/PUC_2469_14/1/.

[26] Joint Helmet Mounted Cueing System, https://www.boeing.com/history/products/joint-helmet-mounted-cueing-system.page#:~:text=The%20Boeing%20Joint%20Helmet%20Mounted%20Cueing%20System%20%28JHMCS%29,sensors%20and%20weapons%20wherever%20the%20pilot%20is%20looking; Helmet Mounted Cueing System (HMCS), https://www.thalesdsi.com/our-services/visionix-2/hmcs/; Joint Helmet Mounted Cueing System (JHMCS), https://elbitsystems.com/product/joint-helmet-mounted-cueing-system-jhmcs/; Joint Helmet Mounted Cueing System, https://www.collinsaerospace.com/what-we-do/Military-And-Defense/Displays-And-Controls/Airborne/Helmet-Mounted-Displays/Joint-Helmet-Mounted-Cueing-System; JHMCS II helmet mounted display system, https://jhmcsii.com.

system in modern military aircraft. Its main task is to deliver reliable information about the pilot's head orientation. This information is then processed in the mission computer to form a set of control signals for a turret gun (or an opto-electronic surveillance system or line of sight or other guided weapon system). Such signals include azimuth and elevation angles.

The magnetic compass and vector magnetometers (e-compass) are the simplest instrument on the aerospace board, but it is subject to a number of errors that must be considered. This applies to both magnetic navigation and helmet systems, including[27]:

- **Magnetic variation (declination)** – in aerial navigation, the angle (difference) on the horizontal plane between the magnetic and true (geographic) directions (meridians). This same angular difference in surveying and land navigation is called declination. The variation error does not change with the heading of the aircraft; it is the same anywhere along the isogonic line.
- **Magnetic deviation** – the angle between compass idle or magnetometer results of north and magnetic north due to presence of local magnetic fields caused by ferromagnetic parts of the object's structure and electrical current. Deviation is different on each heading, but it is not affected by the geographic location and deviation error can be minimized when a pilot or Aviation Maintenance Technicians (AMT) performs the maintenance task known as "swinging the compass".
- **Northerly Turning Errors** (only magnetic compass) – the center of gravity of the float assembly is located lower than the pivotal point. As the airplane turns, the force that results from the magnetic dip causes the float assembly to swing in the same direction that the float turns. The result is a false northerly turn indication. This compass error is amplified with the proximity to either pole.
- **Southerly Turning Errors** (only magnetic compass) – when turning in a southerly direction, the forces are such that the compass float assembly lags rather than leads. The result is a false southerly turn indication. This compass error is amplified with the proximity to either pole.
- **Acceleration Error** (only magnetic compass) – the magnetic dip and the forces of inertia cause magnetic compass errors when accelerating and decelerating on Easterly and westerly headings. When accelerating on either an easterly or westerly heading , the error appears as a turn indication toward north. When decelerating on either of these headings, the compass indicates a turn toward south.
- **Oscillation Error** (only magnetic compass) – oscillation is a combination of all of the other errors, and it results in the compass card swinging back and forth around the heading being flown.
- **Axis non-orthogonality and misalignment, Nonlinearity, Temperature Bias, Hysteresis, Noise** – parameters of vector magnetometers deciding about the quality and reliability of the measurement.

[27] FAA-H-8083-15B Instrument Flying Handbook, U.S. Department of Transportation, Federal Aviation Administration, Flight Standards Service, Oklahoma 2012; SC 063 Sight Compass User Instruction Manual, Doc. P/N: 56-101-01200 Revision E, November 7, 2014, Barfield Inc.

 DOI: 10.55676/asi.v4i2.94

In this paper, there are presented the applications of digital magnetometers in the construction of classical Magnetic Heading Systems (MHS) and modern Helmet Mounted Cueing Systems (HMCS). The focus will be on magnetometer deviation errors and how to minimize them. The theory describing the magnetometer deviation[28] caused by the influence of soft and hard iron (ferromagnets) was taken into account[29]. The aspect of the interaction of direct and alternating electric current, omitted in the classic description of magnetic deviation created in the 19th century, was also indicated. The measurement of the existing deviation (the resultant deviation of the plane and the impact of the compass adjustment correctors) generated by the ferromagnetic elements was carried out in order to verify the correct operation of the HMCS module and the courses with the highest deviation values.

Methodology:

- defining the user's needs and theoretical introduction to problem;
- presentation of the theory of magnetism and deviation;
- methods and measurements;
- data analysis;
- discussion and summary.

2. MATERIALS & METHODS

Before the described tests, the magnetization state of the main ferromagnetic elements of the aircraft was measured (input data for deviation modeling)[30], and in laboratory conditions the properties of the measurement path, including errors in vector magnetometers, were verified using 3D Helmholtz coil. The results from the WMM, EMM and EMAG2 models of the Earth's magnetic field with the magnetic field values on the plane for determining the magnetic deviation were also verified.

The research included:

- **deviation modeling**, taking into account the design features of the aircraft and the parameters of the Earth's magnetic field; a simulation model was developed in the Matlab-Simulink package, using specific mathematical relationships;
- **laboratory tests** of the Helmet Mounted Cueing System and software;
- **airport research** of magnetic deviation on the plane for deviation control, in accordance with the methodology applicable in aviation;
- **verification** of the algorithm during the flight of the aircraft.

[28] Handbook Of Magnetic Compass Adjustment, National Geospatial-Intelligence Agency, Bethesda, MD 2004; Doerfler R, Magnetic Deviation: Comprehension, Compensation and Computation, 2009, http://www.myreckonings.com/wordpress.

[29] Ozyagcilar T., Calibrating an eCompass in the Presence of Hard- and Soft-Iron Interference, Freescale Semiconductor Application Note AN4246, https://www.nxp.com/docs/en/application-note/AN4246.pdf.

[30] Witos M., Zaworski T., Mazurek P., Draganová K., Bogucki K., A Passive Magnetic State Observer in Aviation?, Conference: III International Scientific and Technical Conference 'Safety Management in Techniques, Technologies and Transport Poli-cy', 27 29.11.2019, Szczyrk, DOI: 10.13140/RG.2.2.23244.56965.

The reference criterion is based on the technical assumptions for the MHS and HMSC application. The coefficients in equations (3), (4), (6) and (9) were determined according to the methodology described by Smith (simplified harmonic analysis) and the Discrete Fourier Transform (DFT) analysis.

In the prototype of the Helmet Mounted Cueing System, Figure 3, designed and manufactured in the Air Force Institute of Technology in 2011, two ADIS 16405 iSensor products (Analog Devices company) were incorporated[31], Table 1. The ADIS16405 iSensor is a complete inertial system that includes a triaxial gyroscope, a triaxial accelerometer and a triaxial magnetometer. Each sensor has its own dynamic compensation formulas that provide accurate sensor measurement. Here, the system of helmet position determination is based on the generation of an artificial reference magnetic field "connected" to the aircraft's cockpit.

The main research problem of 3D deviation compensation in aeronautical magnetometers is how to accurately and quickly measure the spatial position of the helmet in the aircraft's coordinate system when the aircraft performing complex figures with a rapid change of the angle of pitch, roll and yaw. The problem involves an interaction between two main coordinate systems:

- 6 the degrees of freedom (DOF) aircraft's system according to the Earth – the position and orientation is defined by three components of translation and three components of rotation;
- 6 DOF helmet's system according to the aircraft

and real time analysis the measurement data of three-axis (3D) magnetometers, accelerometers and gyroscopes from the local coordinate system of sensors, taking into account the external coordinate system, local magnetic anomaly and dynamic of flight. The helmet-mounted system requires many times lower deviation values of the magnetometers than for the compass used in magnetic navigation.

a)

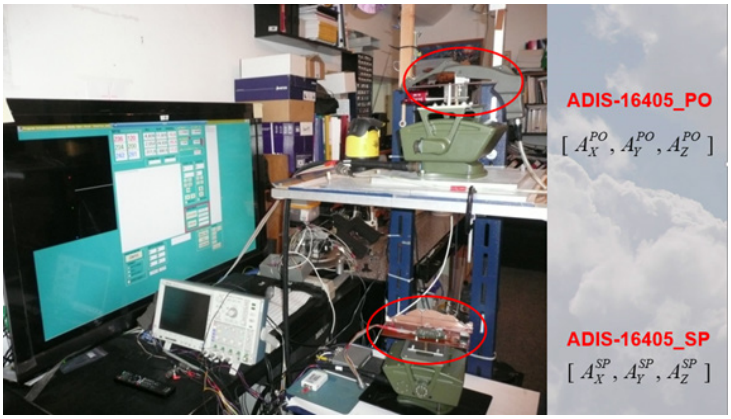

[31] ADIS16405 Triaxial Inertial Sensor with Magnetometer, https://www.analog.com/media/en/technical-documentation/data-sheets/ADIS16405.pdf.

 DOI: 10.55676/asi.v4i2.94

b) 

Figure 3. Laboratory test of ADIS16405 sensors in NSC-1 ORION system: a) deviation test stand of the helmet sensor (ADIS-16405_PO) and the reference sensor (ADIS-16405_SP), b) functional tests

Source: own elaboration.

This research problem is not trivial as it includes metrological and analytical aspects that arise because the pilot is placed inside an aircraft's cockpit, in a weapon system which performs complex and dynamic motions in space and contains ferromagnetic (stationary and rotating) parts and electrical devices (generators, converters, AC and DC avionics systems, propulsion and control systems). Under the influence of operational loads, the stressed ferromagnetic elements change their magnetization.

Example flight parameters of a modern, highly maneuverable aircraft (i.e. F-16, F-22, F-35, MiG-29, Su-37) are values[32]:

- speed: up to 2.2 Ma;
- altitude: up to 12 km above sea level;
- linear accelerations: up to 8 g (78.5 m/s^2);
- angular speeds: up to 1000 degrees/second.

[32] Joint Helmet Mounted Cueing System, https://www.boeing.com/history/products/joint-helmet-mounted-cueing-system.page#:~:text=The%20Boeing%20Joint%20Helmet%20Mounted%20Cueing%20System%20%28JHMCS%29,sensors%20and%20weapons%20wherever%20the%20pilot%20is%20looking; Helmet Mounted Cueing System (HMCS), https://www.thalesdsi.com/our-services/visionix-2/hmcs/; Joint Helmet Mounted Cueing System (JHMCS), https://elbitsystems.com/product/joint-helmet-mounted-cueing-system-jhmcs/; Joint Helmet Mounted Cueing System, https://www.collinsaerospace.com/what-we-do/Military-And-Defense/Displays-And-Controls/Airborne/Helmet-Mounted-Displays/Joint-Helmet-Mounted-Cueing-System; JHMCS II helmet mounted display system, https://jhmcsii.com; Pazur A., Kowalczyk H., Szelmanowski A., A Study on the Existing Helmet-Mounted Display and Control Systems with Respect to the Optimization of Functions and Applications of a Helmet-Mounted Cueing System, Logistyka 6/2011, 3343-3352, https://docplayer.pl/45371329-Analiza-istniejacych-rozwiazan-systemow-nahelmowego-zobrazowania-i-sterowania-dla-optymalizacji-funkcji-i-sposobu.html; Szelmanowski A., Borowski J., Cieślik A., Review of Computer-Assist Methods for the Tracking of the Pilot's Helmet Ori-entation as Applied in the Helmet-Mounted Cueing Systems to Control Military Helicopter's Armament, Logistyka 6/2011, 3633-3640, https://docplayer.pl/158704768-Szelmanowski-andrzej-1-borowski-jerzy-cieslik-andrzej.html; Popowski S., Dąbrowski J., The Method of an Error Validation of Integrated Heading Systems, Measurements. Automation. Robotics, 2015, www.researchgate.net/publication/279217602.

That is why the metrological requirements for a sensor are very demanding. Common demands include:

- update frequency: min. 240 Hz;
- latency: max. 3.5 milliseconds (filter off);
- static accuracy: 0.2 degree RMS for sensor orientation;
- dynamic accuracy: similar to existing solutions.

The system application requires the use of optimized low-band filters in order to minimize errors generated by on-board electrical devices, while maintaining acceptable signal group delays.

Hence, measurement data have to be transferred from a movable head's coordinate system in the form of turret gun control signals – to an immovable turret gun coordinate system affixed within the aircraft. It must be remembered that the turret gun and the pilot's head coordinate systems are not placed in the aircraft's center of gravity, Figure 4. This last determines the flight trajectory and is central to the aircraft coordinate system.

a) b)

Figure 4. Showing: a) location of ID-6 magnetic sensor in Su-22 aircraft (reference sensor for NSC-1 ORION system); b) utilization of a compass rose aids compensation for 2D deviation errors
Source: own elaboration.

The problem of correct determination of the angles of spatial orientation of a pilot's helmet in a helmet mounted cueing systems has many solutions presented in specialist literature and more than 150 patents[33], including through the use of on-board autonomous magnetic field generators and the analysis of differential signals, minimizing the impact of the field generated by the magnetically active elements

[33] Rash C., Helmet Displays in Aviation. Helmet Mounted Display. Design Issues for Rotary-Wing Aircraft, USA, Fort Rucker, 2009; United States Court of Appeals for the Federal Circuit Elbit Systems Of America, LLC, Appellant v. Thales Visionix, INC., Appellee, 2017-1355, http://www.cafc.uscourts.gov/sites/default/files/opinions-orders/17-1355.Opinion.2-5-2018.1.PDF; Pelosi M.J., Patent US7266446B1 Helmet mounted tracking system and method, 2007; Helmet mounting systems, Wilcox Industries Corp. 2007, https://patents.justia.com/patent/8826463.

 DOI: 10.55676/asi.v4i2.94

(hard and magnetic soft iron) of the aircraft. The available scientific publications also introduce the concept of spatial deviation, applicable both in aviation heading systems and in systems for determining the spatial orientation of a pilot helmet with a magnetic method (e.g. using a Helmholtz coil[34]).

One of the basic elements of the error analysis of these systems is the determination of the individual components of the magnetic deviation: circular (impact of the mounting error of the magnetic field sensor in course systems), semi-circular (impact of magnetic hard iron) and quarter-circle (impact of magnetic soft iron) depending on the spatial orientation angles of the airship flying helmet or pilot helmet.

2.1. OBLIGATION TO CONTROL AND COMPENSATE FOR MAGNETIC DEVIATION

In accordance with applicable regulations[35], a compass swing must be performed whenever any ferrous component of the system (i.e. engine frame, transmission, landing gear of the aircraft, flux valve compensator) is installed, removed, repaired or a new compass is installed. Additionally a compass swing must be performed on the following occasions:

- After aircraft has been parked on one heading for over a year;
- When the accuracy of the compass is suspected to be less than 3 degrees;
- After any cockpit modification or major replacement involving ferrous metals;
- When compass has been subjected to shock from a hard landing or turbulence;
- After aircraft has passed through a severe electrical storm;
- After a lightning strike;
- Whenever a change is made to the electrical system;
- Whenever a change of cargo is likely to affect the compass;
- Whenever an aircraft operation is changed to a new geographic location with a major change in magnetic deviation.

2.2. SOFT AND HARD IRON

In the description of magnetic deviation there are the terms “soft iron” and “hard iron”[36].

Soft iron is an iron and other ferromagnets which is instantly magnetised by the approach of a magnetic body or influence the external magnetic field or stress/strain,

[34] Helmholtz Coils, https://ada.nevis.columbia.edu/~zajc/acad/C1494andC2699/eOverm/Helmholtz.htm; Favor E.R., Anderson T., Design of Helmholtz Coil for Low Frequency Magnetic Field Susceptibility Testing, Naval Un-dersea Warfare Center, Division Nevport, USA, 1998.

[35] AC 43-215 - Standardized Procedures for Performing Aircraft Magnetic Compass Calibration Document Information, FAA 2017, https://www.faa.gov/regulations_policies/advisory_circulars/index.cfm/go/document.information/documentID/1031648; SC 063 Sight Compass User Instruction Manual, Doc. P/N: 56-101-01200 Revision E, November 7, 2014, Barfield Inc.

[36] Bozorth R.M., The Physical Basis of Ferromagnetism., Bell System Technical Journal, 1 January 1940, 19, pp 1-39, https://archive.org/details/bstj19-1-1/page/n23/mode/2up; Bozorth R.M., Ferromagnetism. Wiley-VCH, August 1993.

but has no power of retaining magnetism if the energy and physical state of the material has not changed (the level of dislocation, stresses, grain size) – only induced magnetization, $\mathbf{M}_i(\mathbf{H}_e, \mu_{ef})$ where $\mathbf{H}_e$ is the equivalent magnetic field strength; μ_{ef} is the effective magnetic permeability of the material taking into account the influence of the demagnetization tensor (element shape)[37]. Typically ferromagnets with a coercive force $H_c \leq 50\ \mathrm{A/m}$ (the intensity of the Earth's magnetic field), for example, silicon steels used in generators, converters, electromagnets and transformers.

Hard iron is an iron and other ferromagnets which is not magnetized by induction in low magnetic field but which retains a high percentage of the magnetism acquired. In hard iron, the shifting of magnetic domains in low magnetic field of Earths $\mathbf{H}_E$ is irreversible. In other words, the magnetic domains of hard iron do not return to the starting point when magnetic field is removed - the remanent magnetization dominates, $\boldsymbol{M}_r(\mathbf{H}_{e,max}, \mu_{ef})$. Typically ferromagnets with a coercive force $H_c \geq 1000\ \mathrm{A/m}$ for example, pearlitic and martensitic steels used in highly stressed elements, e.g. shafts and axles, bearings, gears, landing gear elements, mounting nodes and alloys used for permanent magnets.

Most ferromagnetic parts on an airplane have a coercivity H_c between $50\ \mathrm{A/m}$ and $1000\ \mathrm{A/m}$, typical of $\alpha - Fe$ ferritic iron and unalloyed, pearlitic and low-alloy steels. In the further considerations, it was assumed that each ferromagnetic element immersed in the Earth's magnetic field with induction $B \approx 50\ 000\ nT$ contains the induced and remanent components of magnetization, $\mathbf{M} = \mathbf{M}_i + \mathbf{M}_r$.

When analysing the problems of magnetic deviation, it should be remembered that ferromagnetic materials do not have a linear relationship between $\mathbf{B}$, $\mathbf{H}$ and $\mathbf{M}$, which is described by equation (1):

$$\mathbf{B} = \boldsymbol{\mu_0}\mathbf{H} + \mathbf{M}\left(\mathbf{H}_{ef}, \frac{\mathbf{H}_{ef}}{\boldsymbol{dt}}\right) \tag{1}$$

where μ_0 is the magnetic permeability of vacuum.

2.3. THE MATHEMATICAL DESCRIPTION OF MAGNETIC DEVIATION

The starting point of MHS and HMCS is the theory of magnetic navigation. The true course is represented by the formula[38]:

$$\textit{True Course} = \textit{Compass Course} \pm \textit{Deviation} = \textit{Magnetic Course} \pm \textit{Variation} \tag{2}$$

Magnetic deviation was analyzed in the 19th century for the navy using magnetic compasses on steel ships. The Scottish mathematician and lawyer Archibald Smith first published in 1843 his equations for the magnetic deviation of a ship - the error in the ship's compasses from permanent and induced magnetic fields in the iron of the ship itself. Determining the magnetic deviation of ships significantly reduced the

[37] Moskowitz R., Della Torre E., Theoretical aspects of demagnetization tensors, IEEE Transactions on Magnetics, 1966, vol. 2, no. 4, pp. 739-744, DOI: 10.1109/TMAG.1966.1065973.

[38] FAA-H-8083-15B Instrument Flying Handbook, U.S. Department of Transportation, Federal Aviation Administration, Flight Standards Service, Oklahoma 2012.

 DOI: 10.55676/asi.v4i2.94

risk of accidents. In the 21st century, the magnetic compass and determining its deviation is mandatory in sea and air transport, despite the use of satellite and ground-based radio navigation.

The Admiralty Manual for the Deviations of the Compass[39] presents in great detail Archibald Smith's derivations of the various equations for magnetic deviation. They are expressed in terms of the ship's magnetic or compass course, the horizontal component and dip of the Earth's magnetic field at a given location, and magnetic parameters unique to a given ship - a three-dimensional (3D) problem that also describes the magnetic deviation of aircraft. A detailed description of the magnetic deviation δ is provided by the *exact equation* (3) and the *inexact equation* (4). The equation (3) provides the deviation using exact coefficient **A**, **B**, **C**, **D** and **E** but is expressed in terms of the non-observable magnetic course. This equation is more useful in characterizing the magnetic properties of ship which can be determined on the basis of static measurements. The equation (4) is expressed in terms of the observable compass course but uses inexact coefficient A, B, C, D, E. The relationships of the terms in the equation (4) is most useful on-ship because at sea or flight the magnetic course ξ is unknown but compass course ξ' is known.

$$\tan\delta = \frac{\mathbf{A} + \mathbf{B}\sin\xi + \mathbf{C}\cos\xi + \mathbf{D}\sin 2\xi + \mathbf{E}\cos 2\xi}{1 + \mathbf{B}\cos\xi - \mathbf{C}\sin\xi + \mathbf{D}\cos 2\xi - \mathbf{E}\sin 2\xi} \tag{3}$$

$$\delta \cong A + B\sin\xi' + C\cos\xi' + D\sin 2\xi' + E\cos 2\xi' \tag{4}$$

where $\delta = \xi - \xi'$ is the magnetic deviation; ξ is the magnetic course; ξ' is the compass course; **A**, **D** and **E** are constants that are dependent only on the arrangement of soft and hard iron in the particular ship; **B** and **C** are constants that are dependent on the Earth's magnetic field at the ship's location as well as the arrangement of its soft and hard iron.

The relationships of the terms in the equation (4) to those in the equation (2) are [40]:

$$A = \arcsin\mathbf{A} \tag{5a}$$

$$B = \arcsin\frac{\mathbf{B}}{1 + 0.5\sin D} \tag{5b}$$

$$C = \arcsin\frac{\mathbf{C}}{1 - 0.5\sin D} \tag{5c}$$

$$D = \arcsin\mathbf{D} \tag{5d}$$

$$E = \arcsin\mathbf{E} \tag{5e}$$

[39] Evans P.J. (Owen F.J.), Smith A., Admiralty Manual for the Deviations of the Compass, Hydrographic Office, Admiralty, London 1869, https://archive.org/details/admiraltymanualforthedeviationsoft/mode/1up.

[40] Ibidem.

The MHS and HMCS applications use three-axis magnetometers, not a compass needle. The three orthogonal components of the Earth's magnetic field are measured, therefore it is useful to use fundamental equations (6a) – (6c) to find the magnetic deviation[41]. These equations were first given by M. Poisson, in the year 1824 in the 5th volume of the Memoirs of the Institute, p. 533.

$$X' = X + aX + bY + cZ + P \tag{6a}$$

$$Y' = Y + dX + eY + fZ + Q \tag{6b}$$

$$Z' = Z + gX + hY + kZ + R \tag{6c}$$

Where the coefficients a, b, c, d, e, f, g, h, k reflect constant parameters – the influence of soft iron and its demagnetization tensor[42], while P, Q, R – the influence of hard iron (constant parameters deduced for a particular ship, reflect the spatial distribution of ferromagnetic masses, their magnetic properties and shape); X is the North component; Y is the East component; Z is the down component; X', Y', Z' represent the components of the combined magnetic force of the Earth and ship in the same directions.

The relationships of the terms in the equations (6) to those in the equation (3) are[43]:

$$\lambda = 1 + \frac{a+e}{2} \tag{7a}$$

$$\mathbf{A} = \frac{d-b}{2\lambda} \tag{7b}$$

$$\mathbf{B} = \frac{1}{\lambda}\left(c \quad \tan\theta + \frac{P}{H}\right) \tag{7c}$$

$$\mathbf{C} = \frac{1}{\lambda}\left(f \quad \tan\theta + \frac{Q}{H}\right) \tag{7d}$$

$$\mathbf{D} = \frac{a-e}{2\lambda} \tag{7e}$$

$$\mathbf{E} = \frac{b+d}{2\lambda} \tag{7f}$$

where at a given location of the ship (latitude, longitude, altitude and time),

$H = \sqrt{X^2 + Y^2}$ is the horizontal component of the Earth's magnetic field;

$\theta = \arctan(Z/H)$ is the dip, or inclination (I), of the Earth's magnetic field;

41 Handbook Of Magnetic Compass Adjustment, National Geospatial-Intelligence Agency, Bethesda, MD 2004; Doerfler R., Magnetic Deviation: Comprehension, Compensation and Computation, 2009, http://www.myreckonings.com/wordpress; Evans P.J. (Owen F.J.), Smith A., Admiralty Manual for the Deviations of the Compass, Hydrographic Office, Admiralty, London 1869, https://archive.org/details/admiraltymanualforthedeviationsoft/mode/1up.

42 Bozorth R.M., The Physical Basis of Ferromagnetism., Bell System Technical Journal, 1 January 1940, 19, pp 1-39, https://archive.org/details/bstj19-1-1/page/n23/mode/2up.

43 Doerfler R., Magnetic Deviation: Comprehension, Compensation and Computation, 2009, http://www.myreckonings.com/wordpress.

 DOI: 10.55676/asi.v4i2.94

λ is parameter deduced for a particular ship, reflect the spatial distribution of ferromagnetic masses, their magnetic properties and shape/demagnetization tensors.

Based on equation (4), the magnetic deviation has at least three components[44], Figure 5:

1. A **constant** term A due to any misalignment of compass north to the ship's keel line (axis of longitudinal symmetry) and to asymmetrical arrangements of soft iron horizontally in the ship.
2. **Semicircular** forces (those with a period equal to 360°):
   - Fore and aft components of the permanent magnetic field due to hard iron and the induced magnetism in asymmetrical vertical iron forward or aft of the compass – the $B \sin \xi'$ term.
   - Athwartship component of the permanent magnetic field due to hard iron and the induced magnetism in asymmetrical vertical iron port or starboard of the compass – the $C \cos \xi'$ term.
3. **Quadrantal** forces (those with a period equal to 180°):
   - Induced magnetism in symmetrical arrangements of horizontal soft iron – the $D \sin 2\xi'$ term.
   - Induced magnetism in asymmetrical arrangements of horizontal soft iron – the $E \cos 2\xi'$ term.

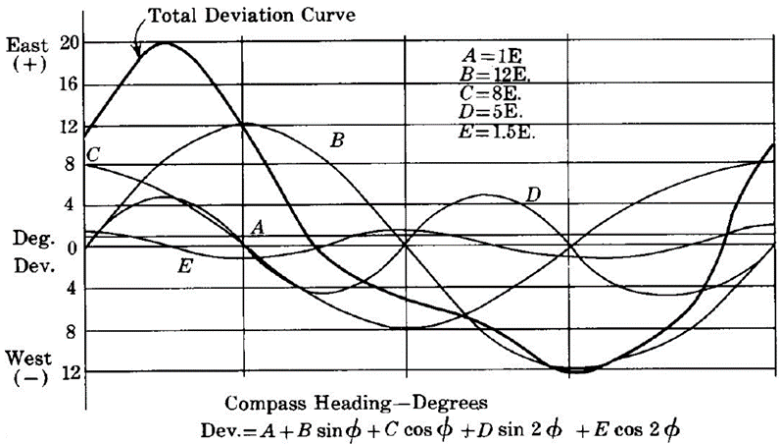

Figure 5. An example of a magnetic deviation of a steel ship – the deviation is more than two times greater than on wooden ships

Source: Evans P.J. (Owen F.J.), Smith A., Admiralty Manual for the Deviations of the Compass, Hydrographic Office, Admiralty, London 1869, https://archive.org/details/admiraltymanualforthedeviationsoft/mode/1up.

[44] Ibidem; Evans P.J. (Owen F.J.), Smith A., Admiralty Manual for the Deviations of the Compass, Hydrographic Office, Admiralty, London 1869, https://archive.org/details/admiraltymanualforthedeviationsoft/mode/1up.

Magnetic deviation is a 3D problem because:

- the coefficients B and C in the equation (3) and (4) depend on the inclination (dip) of the Earth's magnetic field; range of the inclination at the Earth's surface from -90 to +90 degree depending on the location, Figure 6.a);
- the distribution of the magnetic field in the vicinity of soft and hard ferromagnets and the coefficient A, D, E depends on their demagnetization tensor N_{ij} and their position in the Earth's magnetic field, Figure 6. The position-dependent second order demagnetization tensor N_{ij} of the ferromagnetic object can be expressed as an inverse Fourier transform of single function $F(\mathbf{r})$ called the shape function, which encodes the shape of the object, taking the value 1 if $\mathbf{r}$ is inside the object and 0 if $\mathbf{r}$ is outside[45], where $F(\mathbf{k})$ is the Fourier transform of $F(\mathbf{r})$.

$$N_{ij}(\mathbf{r}) = \frac{1}{(2\pi)^3}\int d^3\mathbf{k}\frac{F(\mathbf{k})}{k^2}k_i k_j e^{ik\cdot r} \tag{8}$$

The Smith and Poisson equations were developed before the era of electricity, therefore they do not contain the additional influence of the electric field: the direct current (DC) and alternating current (AC) components present in modern ships and aircraft. Their influence can be included by additional variables $\mathrm{S}, \mathrm{T}, \mathrm{V}$ depending on the instantaneous values of electric current and the position of the circuits on the ship, which is described by equations (9a) – (9c). The value of electric currents in individual circuits may change during movement with a given trajectory. When analyzing precisely the deviation of vector magnetometers and the low-band filtration of their raw measurement signal in HMCS applications, one should also remember about the possible influence of cyclo-stationary components of the magnetic field generated by rotating ferromagnetic elements – values will depend on the operating range of the drive unit.

$$X' = X + aX + bY + cZ + P + S \tag{9a}$$

$$Y' = Y + dX + eY + fZ + Q + T \tag{9b}$$

$$Z' = Z + gX + hY + kZ + R + V \tag{9c}$$

In military aviation, an aircraft performs complex spatial maneuvers during which pitch, roll and yaw angles vary to a large extent. During these maneuvers, the distribution of the scattered magnetic field around all ferromagnetic elements on board changes. Dynamic adjustments are required to obtain reliable results of MHS and HMCS that take into account the magnetic properties, mass, shape and position of the main ferromagnetic elements on board the aircraft and roughly estimated flight parameters.

[45] Lang F., Blundell S.J., Fourier space derivation of the demagnetization tensor for uniformly magnetized objects of cylindri-cal symmetry, Journal of Magnetism and Magnetic Materials 2016, 401, 1060-1067, DOI: 10.1016/j.jmmm.2015.10.133.

 DOI: 10.55676/asi.v4i2.94

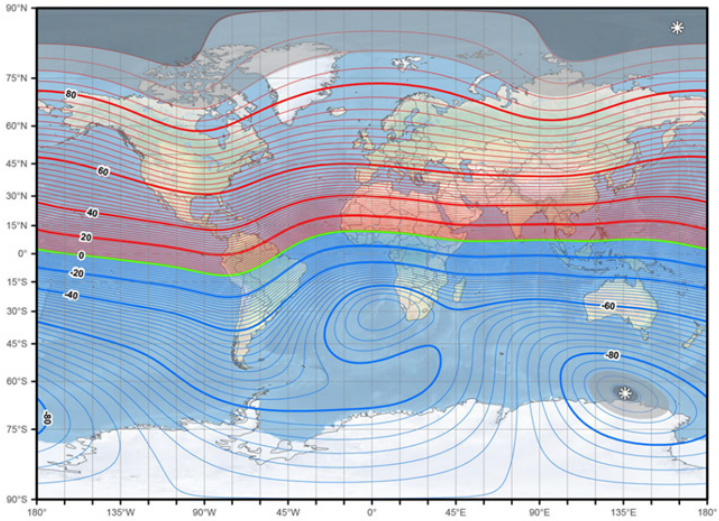

a)

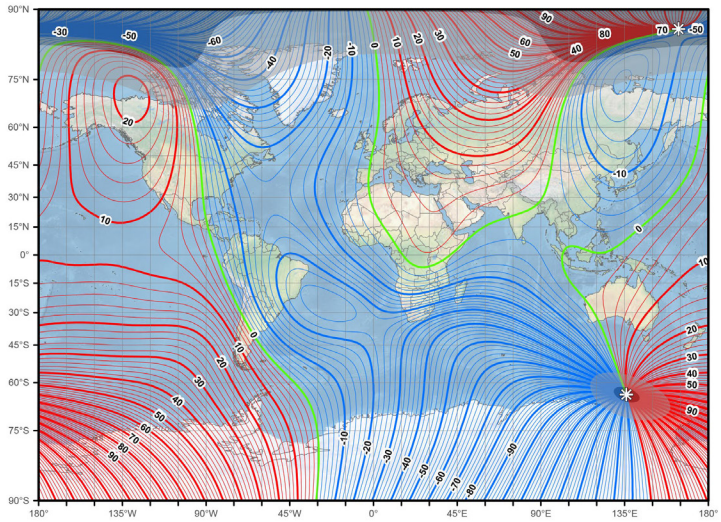

b)

Figure 6. Showing two components of the Earth's magnetic field according to World Magnetic Model for 2020-2025 and Miller projection: a) main field inclination – contour interval is 2 degrees, red contours positive (down); blue negative (up); green zero line; b) main field declination – contour interval is 2 degrees, red contours positive (east); blue negative (west); green zero (agonic) line

Source: Chulliat A., Brown W., Alken P., Beggan C., Nair M., Cox G., Woods A., Macmillan S., Meyer B., Paniccia M., The US/UK World Magnetic Model for 2020-2025: Technical Report, National Centers for Environmental Information, NOAA, 2020. DOI: 10.25923/ytk1-yx35.

2.4. DETERMINING THE HEADING WITH THE USE OF A MAGNETOMETER

To correctly determine the magnetic heading of the aircraft or the spatial orientation of the pilot's helmet with the use of a magnetometer, it is necessary to define the components of the measured magnetic field in the adopted coordinate systems.

The resultant vector of the magnetic field strength seen on the axes of the *S* system related to the aircraft can be written as[46]:

$$\begin{bmatrix} H_x^{SP} \\ H_y^{SP} \\ H_z^{SP} \end{bmatrix} = \begin{bmatrix} H_x^{PM} \\ H_y^{PM} \\ H_z^{PM} \end{bmatrix} + \begin{bmatrix} H_x^{ZT} \\ H_y^{ZT} \\ H_z^{ZT} \end{bmatrix} + \begin{bmatrix} H_x^{ZM} \\ H_y^{ZM} \\ H_z^{ZM} \end{bmatrix}, \tag{10}$$

where:

$\boldsymbol{H_x^{SP}, H_y^{SP}, H_z^{SP}}$ – components of the resultant vector of the magnetic field strength in a place where the magnetometer is installed, seen on the axes of the S system related to the aircraft;

$H_x^{PM}, H_y^{PM}, H_z^{PM}$ – components of the Earth's magnetic field intensity vector at the location of the magnetometer, seen on the axes of the S system associated with the aircraft. It is a vector without distorting the Earth's magnetic field;

$\boldsymbol{H_x^{ZT}, H_y^{ZT}, H_z^{ZT}}$ – components of the resultant magnetic field strength vector from magnetic hard iron, in a place where the magnetometer is installed, seen on the axes of the S system associated with the aircraft. This vector distorts the Earth's magnetic field when exposed to magnetic hard iron;

$\boldsymbol{H_x^{ZM}, H_y^{ZM}, H_z^{ZM}}$ – components of the magnetic field strength vector from magnetic soft iron, in a place where the magnetometer is installed, seen on the axes of the S system related to the aircraft.

The components of the Earth's magnetic field intensity vector at the location of the magnetometer, seen on the axes of the S system associated with the aircraft, are complex functions of many parameters[47]:

$$\begin{aligned} H_x^{PM} &= f(\Psi_{wz}^M, \Theta, \Phi, \gamma_{PM}, H^{PM}) \\ H_y^{PM} &= f(\Psi_{wz}^M, \Theta, \Phi, \gamma_{PM}, H^{PM}) \\ H_z^{PM} &= f(\Psi_{wz}^M, \Theta, \Phi, \gamma_{PM}, H^{PM}) \end{aligned} \tag{11}$$

where:

Ψ_{wz}^{PM} – aircraft yaw angle measured in the horizon plane, relative to the magnetic meridian (magnetic heading);

Θ – aircraft pitch angle;

Φ – aircraft roll angle;

γ_{PM} – inclination of the Earth's magnetic field strength vector;

H^{PM} – vector module of the Earth's magnetic field strength.

[46] Witos M., Szelmanowski A., Pazur A., Borowski J., Research on errors of magnetic field sensors and algorithms for de-termining 3D spatial deviation in aeronautical heading reference systems, 2021 IEEE 8th International Workshop on Me-trology for AeroSpace (MetroAeroSpace), 23-25 June 2021, pp. 25-30, DOI: 10.1109/MetroAeroSpace51421.2021.9511761.

[47] Ibidem.

 DOI: 10.55676/asi.v4i2.94

The components of the magnetic field strength vector from hard iron in the place where the magnetometer is installed, seen on the axes of the S system related to the aircraft, are complex functions of many parameters[48]:

$$\begin{aligned} H_x^{ZT} &= f(\delta_{ZT}, \gamma_{ZT}, H^{ZT}) \\ H_y^{ZT} &= f(\delta_{ZT}, \gamma_{ZT}, H^{ZT}) \\ H_z^{ZT} &= f(\delta_{ZT}, \gamma_{ZT}, H^{ZT}) \end{aligned} \tag{12}$$

where:

δ_{ZT} – declination of the vector of the resultant magnetic field strength due to magnetic hard iron in the S system associated with the aircraft;

γ_{ZT} – inclination of the vector of the resultant magnetic field strength due to magnetic hard iron in the S system associated with the aircraft;

H^{ZT} – vector modulus of the resultant magnetic field strength from magnetic hard iron.

The components of the soft iron magnetic field strength vector in the place where the magnetometer is installed, seen on the axes of the S system related to the aircraft, are complex functions of many parameters[49]:

$$\begin{aligned} H_x^{ZM} &= f\left(\Psi_{wz}^M, \Theta, \Phi, H_x^{PM}, H_y^{PM}, H_z^{PM}\right) \\ H_y^{ZM} &= f\left(\Psi_{wz}^M, \Theta, \Phi, H_x^{PM}, H_y^{PM}, H_z^{PM}\right) \\ H_z^{ZM} &= f\left(\Psi_{wz}^M, \Theta, \Phi, H_x^{PM}, H_y^{PM}, H_z^{PM}\right) \end{aligned} \tag{13}$$

where:

δ_{ZM} – declination of the vector of the resultant magnetic field strength from magnetic soft iron in the S system associated with the aircraft;

γ_{ZM} – inclination of the vector of the resultant magnetic field strength from magnetic soft iron in the S system associated with the aircraft.

2.5. THE VECTOR OF THE STRENGTH OF THE EARTH'S MAGNETIC FIELD ANALYZED ON THE AXES OF THE SYSTEM RELATED TO THE AIRCRAFT

From the geometric dependencies presented in, the projection modules of the Earth's magnetic field intensity vector on the axes of the M system are given by the equation[50]:

$$\begin{bmatrix} H_{xm}^{PM} \\ H_{ym}^{PM} \\ H_{zm}^{PM} \end{bmatrix} = \boldsymbol{MT}_1 \times \begin{bmatrix} H^{PM} \\ 0 \\ 0 \end{bmatrix} \tag{14}$$

where:

$H_{xm}^{PM}, H_{ym}^{PM}, H_{zm}^{PM}$ – components of the Earth's magnetic field strength vector in a normal M system associated with the Earth with an aircraft origin;

48 Ibidem.
49 Ibidem.
50 Ibidem.

$\boldsymbol{MT_1}$ – transformation matrix from the H system related to the Earth's magnetic field vector to the S system related to the aircraft.

The components of the magnetic field vector of the M system seen on the axes of the S system related to the aircraft are given by the equation[51]:

$$\begin{bmatrix} H_x^{PM} \\ H_y^{PM} \\ H_z^{PM} \end{bmatrix} = \boldsymbol{MT} \downarrow_S^M \times \begin{bmatrix} H_{xm}^{PM} \\ H_{ym}^{PM} \\ H_{zm}^{PM} \end{bmatrix} \tag{15}$$

where:

$H_{xm}^{PM}, H_{ym}^{PM}, H_{zm}^{PM}$ – components of the Earth's magnetic field strength vector in the system associated with the aircraft;

$\mathbf{MT} \downarrow_S^M$ – transformation matrix from normal M system to S system related to the aircraft.

2.6. THE MAGNETIC FIELD VECTOR FROM HARD MAGNETIC IRON ANALYZED ON THE AXES OF THE SYSTEM RELATED TO THE AIRCRAFT

The magnetic field of hard magnetic iron on aircraft does not change its position with respect to the axis of the coordinate system associated with the aircraft. This field, in relation with the Earth's magnetic field, weakens or strengthens the resultant magnetic field depending on the mutual position of the intensity vectors of these fields. As a result, this causes an error in the magnetic heading indication, called the semicircular deviation, which takes the value of zero twice for a complete revolution of the aircraft in the horizontal plane.

From the geometric dependencies of the projections of the magnetic field intensity vector from hard magnetic iron on the axes of the system S presented in modules, the following dependence is given[52]:

$$\begin{aligned} H_x^{ZT} &= H^{ZT} \cdot cos(\gamma_{ZT}) \cdot cos(\delta_{ZT}) \\ H_y^{ZT} &= H^{ZT} \cdot cos(\gamma_{ZT}) \cdot sin(\delta_{ZT}) \\ H_z^{ZT} &= -H^{ZT} \cdot sin(\gamma_{ZT}) \end{aligned} \tag{16}$$

where:

$H_x^{ZT}, H_y^{ZT}, H_z^{ZT}$ – components of the magnetic field strength vector for hard iron magnetically in the S system of coordinates associated with the aircraft;

H^{ZT} – vector module deflecting the Earth's magnetic field from magnetic hard iron;

δ_{ZT} – declination of the deflection vector in the S system;

γ_{ZT} – inclination of the deflection vector in the S system.

[51] Ibidem.
[52] Ibidem.

 DOI: 10.55676/asi.v4i2.94

2.7. THE MAGNETIC FIELD VECTOR FROM HARD MAGNETIC IRON ANALYZED ON THE AXES OF THE SYSTEM RELATED TO THE AIRCRAFT

The magnetic field from soft magnetic iron on board the aircraft changes its position in relation to the axis of the S system. The direction of magnetization of magnetic domains from soft iron is consistent with the direction of the Earth's magnetic field, while the opposite direction is opposite. The magnetic field strength vector created in this way affects the Earth's magnetic field strength vector, distorting the magnetic field force lines at the point of measurement with a magnetometer. The measuring system, by measuring the components of the resultant magnetic field intensity, will measure along with the errors of the quadrantal magnetic deviation.

This vector, interacting with the vector of the Earth's magnetic field, also weakens or strengthens the resultant field, depending on the relative position of these vectors. As a result, this causes an error called quadrantal deviation, which is determined in the horizontal plane (for $\Theta = 0$ and $\Phi = 0$) to zero, four times per complete revolution of the aircraft.

From the geometrical dependencies presented in the projection modules of the magnetic field strength vector from soft magnetic on the axes of the system S are given by the relationship[53]:

$$\begin{bmatrix} H_x^{ZM} \\ H_y^{ZM} \\ H_z^{ZM} \end{bmatrix} = \begin{bmatrix} D_1 \\ D_2 \\ D_3 \end{bmatrix} + \begin{bmatrix} D_{11} & D_{12} & D_{13} \\ D_{21} & D_{22} & D_{23} \\ D_{31} & D_{32} & D_{33} \end{bmatrix} \times \begin{bmatrix} H_x^{PM} \\ H_y^{PM} \\ H_z^{PM} \end{bmatrix} \tag{17}$$

where:

H_x^{ZM}, H_y^{ZM}, H_z^{ZM} – components of the resultant vector of magnetic field strength for soft magnetic iron in the S system of coordinates associated with the aircraft;

D_1, D_2, D_3 – constant components of the magnetic field strength vector from magnetic soft iron;

$D_{11} \div D_{33}$ – coefficients for the variable components of the magnetic field strength vector from magnetic soft iron.

3. RESULTS

Presentation of the method of determining the components of magnetic deviation, selected studies of the influence of magnetometer positioning errors and the study of magnetic deviation in the horizontal plane (2D deviation performed at the airport) and in three-dimensional space (3D deviation used, among others in helmet systems) are presented.

[53] Ibidem.

3.1. MEASUREMENTS OF THE SCATTERING FIELD IN THE VICINITY OF FERROMAGNETIC OBJECTS

The aim of the preliminary research was to assess the level of magnetic field disturbances generated by stationary and moving ferromagnetic objects aboard the aircraft and the possibility of modeling them using a simplified model of a magnetic dipole (with the criterion of observation distance greater than 3 lengths of the characteristic sources of disturbances). It has been found that the landing gear of the aircraft, large ferromagnetic elements of the power unit and electric generators generate a local magnetic field that may be many times greater than the Earth's magnetic field[54]. It was also found that this component of the magnetic field can be used for non-contact diagnostics of critical components of the aircraft and for the identification of operational exceedances not recorded directly by on-board recorders.

3.2. MAGNETIC DEVIATION OF SU-22 FIGHTERS

The existing magnetic deviation (from 2005-2021) of Su-22 aircraft operated by the Polish Armed Forces was analyzed statistically based on measurement data for 8 points (aircraft magnetic courses). The magnetic deviation control was performed with the engine and electrical equipment off. The statistical pattern for the complete population of airplanes is shown in Figure 7. It was found that the average magnetic deviation of the Su-22 aircraft population has a clear maxima at 135 and 315 degrees and minima at 45 and 225 degrees. The standard deviation shows a circular asymmetry with a clear shift towards the North. The average values of the magnetic deviation coefficients show the dominant influence of D, A and B, and the negligible influence of E. The standard deviation (a measure of differentiation of the deviation values observed between airplane) reveals the dominant influence of the A, B and C coefficients.

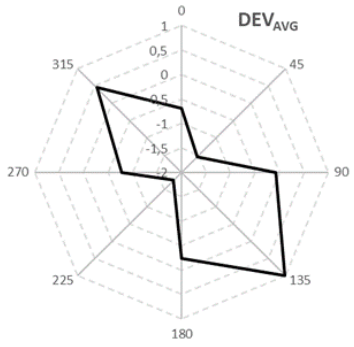

a)

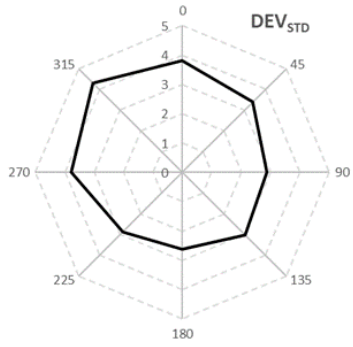

b)

54 Ibidem.

 DOI: 10.55676/asi.v4i2.94

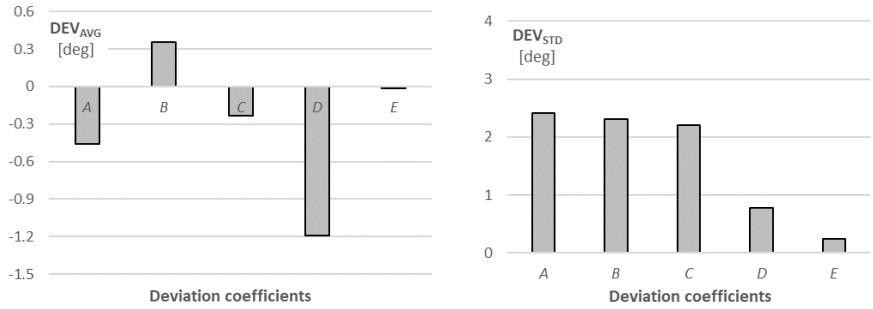

c) d)

Figure 7. Statistical analysis of the magnetic deviation of the Su-22 aircraft population compasses

Source: own elaboration.

Then the methodology of magnetic deviation compensation (measure was verified at 8, 4 and 24 points. The applied methodology enables to obtain the residual magnetic deviation not exceeding the value of **5 arc minutes** (1.54 mrad). After fine adjustment of compass, the magnetic deviation did not exceed **3 degrees** (52.4 mrad) during the flight with roll and pitch angles up to 20 degrees.

3.3. SIMULATION MODEL FOR THE DETERMINATION OF 2D AND 3D MAGNETIC DEVIATION

The simulation model developed at AFIT, Figure 8 allows for the determination of individual components of magnetic deviation on the basis of the modeled, spatial distribution of the disturbance vectors of the Earth's magnetic field.

The model takes into account the spatial location of the magnetic field intensity vector depending on the longitude and latitude of the measurement site.

The model determines the distortions of the magnetic field from hard magnetic iron, which results in a semi-circular deviation, included in the B and C coefficients. The spatial distribution of the magnetic field distortion vector, determined for soft magnetic iron, gives us a quarter-circle deviation, taken into account in the coefficients D and E. Simulation model for the determination of 2D and 3D deviation.

An important element of the developed simulation model is the spectral analysis module, used to generate the spectral distribution of the total magnetic deviation course, treated as a periodic function (with a period of 360 degrees).

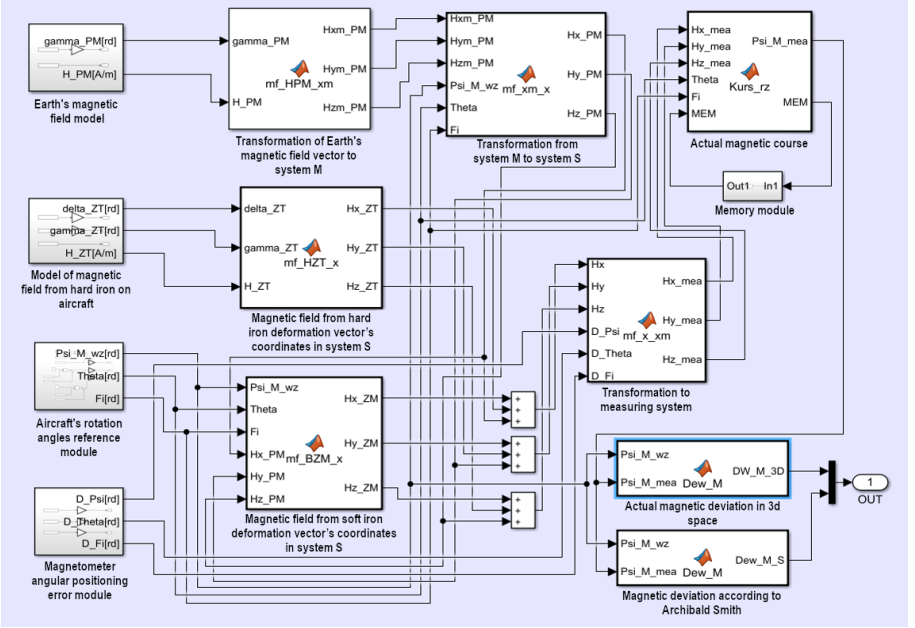

Figure 8. Simulation model for the determination of 2D and 3D deviation

Source: Witos M., Szelmanowski A., Pazur A., Borowski J., Research on errors of magnetic field sensors and algorithms for de-termining 3D spatial deviation in aeronautical heading reference systems, 2021 IEEE 8th International Workshop on Me-trology for AeroSpace (MetroAeroSpace), 23-25 June 2021, pp. 25-30, DOI: 10.1109/MetroAeroSpace51421.2021.9511761.

3.4. INVESTIGATION OF THE INFLUENCE OF MAGNETOMETER POSITIONING ERRORS

The inaccurate alignment of the magnetometer measurement axes with respect to the axis of the system related to the aircraft affects the magnetometer positioning errors.

The resultant magnetic field in the measurement system can be represented by the relationship[55]:

$$\begin{bmatrix} H_x^{MEA} \\ H_y^{MEA} \\ H_z^{MEA} \end{bmatrix} = \boldsymbol{MT} \downarrow_P^S \times \begin{bmatrix} H_x^{SP} \\ H_y^{SP} \\ H_z^{SP} \end{bmatrix} \tag{18}$$

where:

$H_x^{MEA}, H_y^{MEA}, H_z^{MEA}$ – components of the Earth's magnetic field strength vector in the measuring P system;

$\boldsymbol{MT} \downarrow_P^S$ – transformation matrix from normal S system to P system related to the magnetometer;

55 Ibidem.

 DOI: 10.55676/asi.v4i2.94

$\Delta\Phi$ – positioning error in the roll of the magnetometer;

$\Delta\Theta$ – positioning error in the pitch of the magnetometer;

$\Delta\Psi$ – positioning error in the yaw of the magnetometer.

3.5. RESEARCH ON MAGNETIC DEVIATION IN THE 2D HORIZONTAL DEVIATION

2D horizontal deviation is determined for classical (gimbal) heading systems using the Earth's magnetic field. Horizontal deviation is defined as the difference between the magnetic heading measured in the measurement system and the reference magnetic heading, resulting from the precise, geometric alignment of the longitudinal axis of the aircraft (e.g. on the deviation circle / compass rose).

Such deviation is usually determined for the selected values of the magnetic heading when the aircraft is positioned in the horizontal plane (Θ = 0 and Φ = 0). This is a horizontal deviation, denoted as 2D and described as follows[56]:

$$DW^{2D} = \Psi_{mea}^{M2D} - \Psi_{wz}^{M} \tag{19}$$

where:

$$\Psi_{mea}^{M2D} = arctg\left[\frac{-H_y^{MEA}}{H_x^{MEA}}\right]$$

For its description, the simplified 2D magnetic deviation dependence according to the formula (4) of A. Smith is often used.

$$D^{2D}(\Psi_{wz}^{M}) = A + B \cdot sin(\Psi_{wz}^{M}) + C \cdot cos(\Psi_{wz}^{M}) + D \cdot sin(2 \cdot \Psi_{wz}^{M}) + E \cdot cos(2 \cdot \Psi_{wz}^{M}) \tag{20}$$

where:

$D^{2D}(\Psi_{wz}^{M})$ – measured deviation values at individual magnetic courses;

A – circular deviation as a sensor assembly error;

B, C – components of semicircular deviation (first harmonic in the course of total deviation);

D, E – components of a quadrantal deviation (second harmonic in the course of total deviation).

3.6. RESEARCH ON MAGNETIC DEVIATION IN 3D SPACE DEVIATION

Magnetic deviation determined for any values of pitch and roll angles of the aircraft is a 3D spatial deviation. The 3D deviation is determined for cardan-free heading systems that use magnetometers built into the system related to the aircraft or the pilot's helmet (e.g. in HMCS systems).

[56] Ibidem.

Based on the previously presented mathematical relationships, the 3D deviation can be presented as follows[57]:

$$DW^{3D} = \Psi_{mea}^{M3D} - \Psi_{wz}^{M} \tag{21}$$

where:

$$\Psi_{mea}^{M3D} = arctg\left[\frac{H_z^{MEA} \cdot \sin\Phi - H_y^{MEA} \cdot \cos\Phi}{H_x^{MEA} \cdot \cos\Theta + H_y^{MEA} \cdot \sin\Theta \cdot \sin\Phi + H_z^{MEA} \cdot \sin\Theta \cdot \cos\Phi}\right] \tag{22}$$

By introducing the values of the deviation coefficients, describing the structural elements for a given type of aircraft, hard iron and soft magnetic iron, it is possible to determine individual errors of indications of the measurement system using the Earth's magnetic field.

4. DISCUSSION

Modern digital and analog magnetometers have a wider bandwidth than a compass and greater sensitivity (sub-pT, pT, nT). They also record unwanted signals that have the characteristics of stochastic color noise (pink, red, white, …) and deterministic signals e.g. 50 / 60Hz, 115Hz, 400Hz network component and their odd harmonics and cyclo-stationary disturbances generated by rotating ferromagnetic elements. Signal components that can be used in structural health monitoring systems and pro-active prevention.

The performed tests allowed to identify the sources of errors in measurement of magnetic field caused by the influence of:

- the local magnetic field generated by active elements of the aircraft (ferromagnets and electrical circuits) and
- simplified methodology (maximum 32 aircraft angular positions within one revolution about the vertical axis) and used equation (4) - expansion of equation (3) into an additive form containing only one term of the Taylor series, omitting very weak components (results of multiplication of the trigonometric functions of sines and cosines) for determining deviation;
- magnetic field generated by electrical systems of AC and DC currents.

When the deviations much exceed 20°, and great accuracy is required, these coefficients are represented by **A**, **B**, **C**, **D**, **E** in the equation (3) – in navigation books the letters of the German alphabet at Smith's methodology[58]. The Roman letters from the equation (4) represent a certain number of degrees and minutes; the German letters represent the natural sines (nearly) of the arcs of the corresponding Roman letters.

[57] Ibidem.

[58] Evans P.J. (Owen F.J.), Smith A., Admiralty Manual for the Deviations of the Compass, Hydrographic Office, Admiralty, London 1869, https://archive.org/details/admiraltymanualforthedeviationsoft/mode/1up.

 DOI: 10.55676/asi.v4i2.94

The presented simulation model also allows for the study of magnetic deviation not only in the horizontal plane (at the corners Θ = 0 and Φ = 0) but also over a wide range of aircraft pitch and roll changes.

4.1. DEVIATION STUDIES FOR PITCH AND COURSE CHANGES

The research showed that the inaccurate alignment of the magnetometer measurement axes in relation to the longitudinal price of the aircraft causes changes in exhaust deviation in the pitch and course channel.

An exemplary course of changes in 3D magnetic deviation at different values of pitch angles and aircraft heading is shown in Figure 9. The assumed range of pitch angle changes is from $-\pi/2$ do $+\pi/2$, a course from 0 to 2π (at a heel angle equal to 0).

The analysis of the obtained course in the form of contour lines, Figure 10 showed the occurrence of local extremes, the maximum values of which do not exceed **0.20 rad** (11.46 degree). This value is slightly higher than for wooden sea vessels.

The spectral analysis of the obtained total deviation waveforms, with the use of the Toolbox FFT module in the Matlab-Simulink environment, for the adopted range of tilt angle and course changes, showed that the dominant component is close to the quadrantal deviation component. Compensation of this influence can be implemented by software or by means of a specialized magnetic compensator.

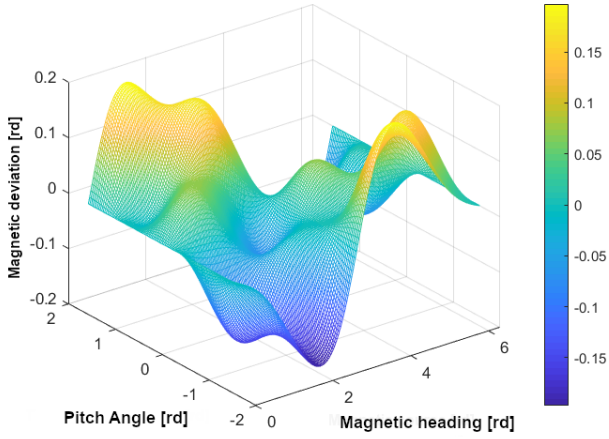

Figure 9. Exemplary 3D magnetic deviation for the aircraft's model when changing the pitch angle and magnetic heading (before deviation compensation)

Source: Witos M., Szelmanowski A., Pazur A., Borowski J., Research on errors of magnetic field sensors and algorithms for de-termining 3D spatial deviation in aeronautical heading reference systems, 2021 IEEE 8th International Workshop on Me-trology for AeroSpace (MetroAeroSpace), 23-25 June 2021, pp. 25-30, DOI: 10.1109/MetroAeroSpace51421.2021.9511761.

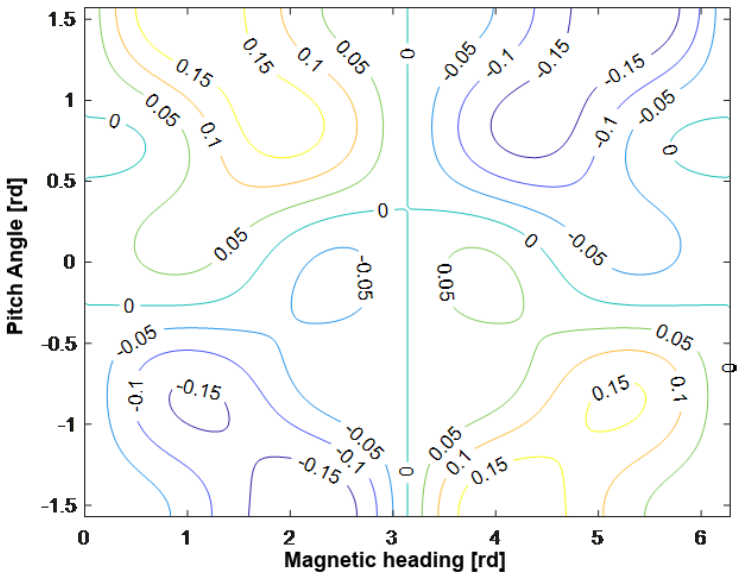

Figure 10. Example of 3D magnetic deviation for the aircraft's model when changing the pitch angle and magnetic heading (before deviation compensation)

Source: own elaboration.

4.2. DEVIATION STUDIES FOR TILT AND COURSE CHANGES

The performed tests showed that the inaccurate alignment of the magnetometer measurement axes in relation to the lateral axis of the system related to the aircraft causes changes in the total deviation in the tilt and course channel.

The exemplary waveforms of changes in 3D magnetic deviation at different values of tilt angles and aircraft heading are shown in Figure 11. The assumed range of changes in the tilt angle is from $-\pi$ do $+\pi$, a course from 0 to 2π (at an angle of inclination equal to 0).

The analysis of th e obtained course in the form of contour lines, Figure 12 showed the occurrence of local extremes, the maximum values of which do not exceed **0.20 rad** (11.46 degree). This value is slightly higher than for wooden sea vessels.

The presented error courses of indications Figure 9, Figure 10, Figure 11 and Figure 12 show that the change of the aircraft pitch and roll angles significantly influences the errors of the magnetic heading measurement. Compensation for magnetic deviation, defined only in the horizontal plane, may not be sufficient for aircraft maneuvering with large changes in pitch and tilt angles.

The distribution of the magnetic field disturbing the measurement on each aircraft may be different. Therefore, it is expedient to perform the magnetic deviation compensation taking into account the changes of the pitch and roll angles.

 DOI: 10.55676/asi.v4i2.94

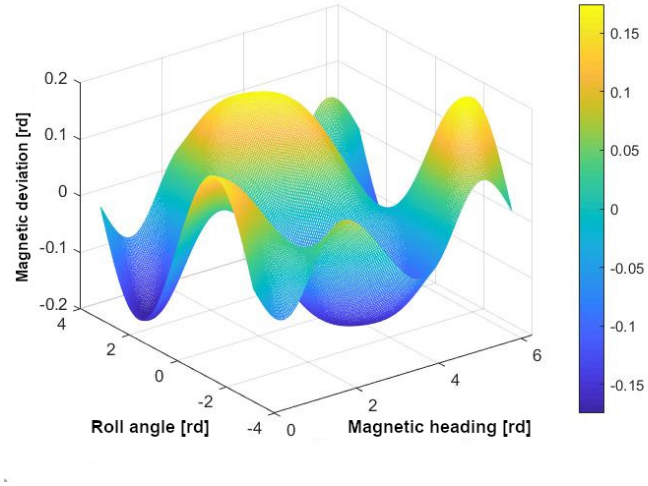

Figure 11. 3D magnetic deviation for the aircraft's model when changing the roll angle and magnetic heading (before deviation compensation)

Source: Witos M., Szelmanowski A., Pazur A., Borowski J., Research on errors of magnetic field sensors and algorithms for de-termining 3D spatial deviation in aeronautical heading reference systems, 2021 IEEE 8th International Workshop on Me-trology for AeroSpace (MetroAeroSpace), 23-25 June 2021, pp. 25-30, DOI: 10.1109/MetroAeroSpace51421.2021.9511761.

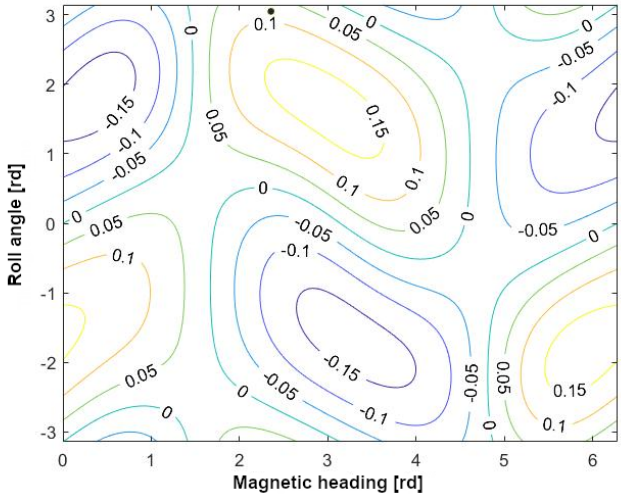

Figure 12. 3D magnetic deviation for the aircraft's model when changing the roll angle and magnetic heading (before deviation compensation)

Source: own elaboration.

4.3. HARMONIC ANALYSIS OF MAGNETIC DEVIATION

The classical algorithm of deviation component analysis according to A. Smith's methodology is sufficient to ensure safe magnetic navigation and MHS application. Smith's methodology may not be sufficient for HMCS because the measurement uncertainty of the helmet position relative to the aircraft coordinate system is the sum of the deviations of the two magnetometers: the helmet and the aircraft. For these applications it is advisable to use formula (3) and dynamic correction taking into account additional components generated by AC and DC electric current. It is also advisable to analyze higher harmonic deviations using the DFT algorithm. An exemplary result of the harmonic analysis is shown in Figures 13 and 14. The results reflect the resultant influence of the magnetic field of the Earth and the aircraft (the unobservable effort of the structure and the technical condition of the ferromagnetic and meta-stable paramagnetic components) as well as the influence of the deviation compensation system and the technical condition of the compass.

For the population of Su-22 the signal of magnetic deviation is dominated by:

- **Human errors** related to the constant deviation coefficient A - non-axial mounting of the compass transmitter on the plane or asymmetrical arrangements of soft iron horizontally in the plane; this component has been reduced more than 80% by additional training of personnel performing the installation of the compass transmitter and deviation, as well as Air Force Institute of Technology supervision over deviation at the repair plant and air bases;
- **Semicircular magnetic deviation** - first harmonic order (1x) of B and C deviation coefficients - components of the permanent magnetic field due to hard iron and the induced magnetism in asymmetrical vertical iron forward or aft of the compass;
- **Quadrantal magnetic deviation** – only second harmonic order (2x) of D deviation coefficient - induced magnetism in symmetrical arrangements of horizontal soft iron; coefficient E is negligible - induced magnetism in asymmetrical arrangements of horizontal soft iron.

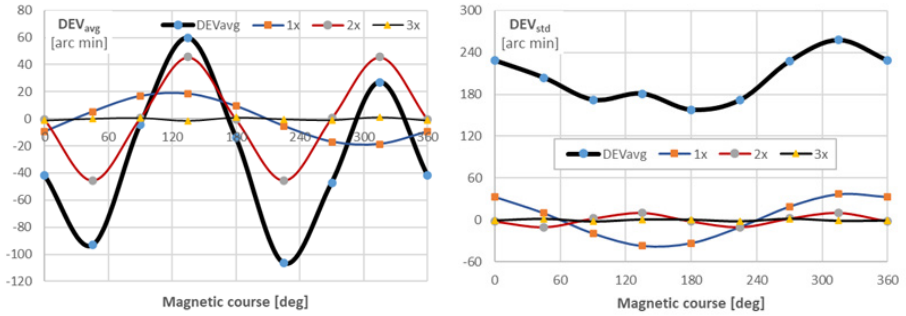

 DOI: 10.55676/asi.v4i2.94

Deviation coefficient	DEV_{avg}	1x	2x	3x	DEV_{std}	1x	2x	3x
	[arc min]				[arc min]			
A	-29.02	-1.04	-0.07	-0.12	**203.17**	3.68	-0.23	-0.05
B	21.41	**16.92**	0.00	0.79	-27.39	-19.43	0.00	**-1.74**
C	-13.90	-9.36	0.00	**-1.05**	35.24	**33.13**	0.00	-0.47
D	**-71.71**	0.00	**-45.53**	0.00	-15.74	0.00	**-10.02**	0.00
E	-1.04	0.00	-0.66	0.00	-3.23	0.00	-2.06	0.00

Figure 13. Diagrams shows analyzed signal in relation to course. Table shows harmonic analysis of the statistical pattern of magnetic deviation of the Su-22 population (input data as in the Figure 7; DEV_{avg} is the mean value of the magnetic deviation in the Su-22 population at the given magnetic rate; DEV_{std} is the standard deviation of magnetic deviation in the Su-22 population at the given magnetic heading) in relation to harmonics. The values marked bold are highest and lowest values for a given harmonics

Source: own elaboration.

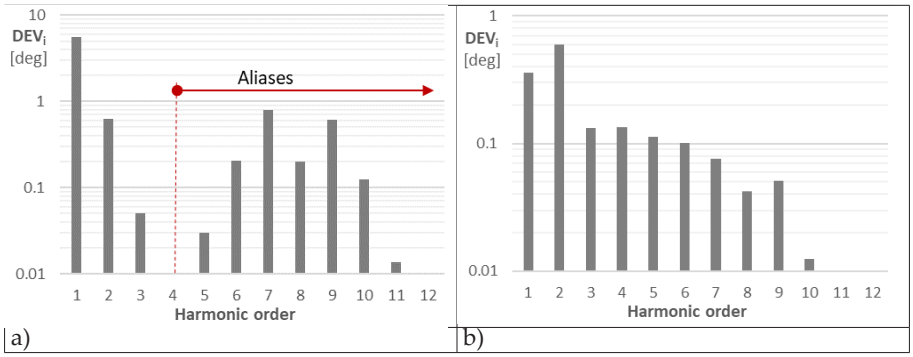

Figure 14. Harmonic spectrum of magnetic deviation on the Su-22 aircraft: a) the input state before compass adjustment (control in 8 points / magnetic courses); b) the impact of removing the dominant component of magnetic deviation with (a) - the state before accurate compass adjustment at 24 points / magnetic courses of the aircraft (spectrum up to 12 harmonic without aliases)

Source: own elaboration.

After the initial compass adjustment, the constant deviation coefficient A and the deviation coefficients B and C (1st harmonic order) was reduced, which is confirmed by the measurement at 24 points / courses of the plane, Figure 14.b). After fine adjustment, the residual magnetic deviation of compass does not exceed 2 arc minutes. The spatial location of ferromagnetic elements on the plane and the change in the position of some of them, e.g. the main landing gear and the front landing gear, causes the magnetic deviation to increase to 2-3 degrees during horizontal flight. The deviation also increases when performing higher pilot figures, which is important for the helmet system. Dynamic compensation of magnetic deviation errors is possible with the described algorithm.

The third and higher harmonics of the magnetic deviation are lower than the compass resolution – it is noticeable only in statistical data and in the pT and nT measurement data of magnetometers in helmet systems.

On the basis of the 3 sigma criterion, it was estimated that less than 2.5% of airplanes may have exceeded the allowable magnetic deviation between consecutive inspections and adjustments of the compass compensation system. Central monitoring of the level of magnetic deviation reduces the risk of operating an aircraft with a defective compass, which directly translates into flight safety. It is also possible to diagnose the level of human errors and undertake effective prevention.

5. CONCLUSIONS

The presented operational problems, theoretical issues of magnetic navigation and the study of the error of magnetic deviation in the navigation systems of the Su-22 aircraft and helmet-mounted systems confirmed the purposefulness of analyzing the 3D problem.

The conducted research allowed for the development of a description and verification of measurement algorithms for the determination of 2D horizontal deviation and 3D spatial deviation occurring during aircraft maneuvers for variable pitch, roll and yaw (magnetic course) angles.

The static characteristics determined in the simulation model, in the form of 2D horizontal deviation waveforms, can be a source of diagnostic information on the structural health of the course system, magnetic field sensor, magnetic corrector, calculator and navigation data presentation system of each aircraft.

With regard to the standard approach presented by manufacturers of magnetometers, it should be emphasized that the mathematical models and algorithms they provide for the identification and calibration of 3D deviation confirm the following properties:

- it is possible to calibrate the measuring system using magnetometers by a user who has no previous knowledge of the location of the measuring system or the direction of magnetic north;
- the magnetometer readings are affected by soft and hard iron disturbances caused by the use of ferromagnetic materials on the printed circuit board on the ellipsoid surface. These indications can be accurately modeled with 10 parameters determined in the calibration process;
- the measurement system calibration process consists in adjusting the adopted 10-parameter model to the indications of magnetometers, in which there is a 3-parameter model of displacement of indications from the influence of hard iron, a 6-parameter matrix of the influence of soft iron and a 1-parameter model of geomagnetic field induction;
- knowing the 10-parameter model, it is possible to transform the magnetometers' indications from the position on the surface of the ellipsoid to the position on the surface of the sphere centered in the center using a simple programmatic

 DOI: 10.55676/asi.v4i2.94

procedure. This transformation removes the disturbances caused by the influence of hard and soft iron, allowing the calculation of the exact value of the magnetic heading.

With regard to the approach used in AFIT, it should be emphasized that the developed mathematical model and algorithms for identifying and calibrating 3D deviations confirm the following properties:

- it is possible to calibrate the measuring system with the use of magnetometers by the user having prior knowledge of the calibration coefficients (determined in the process of periodic deviation works);
- the developed method of identifying 3D deviation is based on a 15-parameter mathematical model, in which 3 parameters define the influence of hard iron, and 12 parameters define the influence of soft iron;
- this method can be used in AHRS and INS (magnetic channel) airline magnetic heading systems.

The unquestionable advantage of vector magnetometers measuring the three orthogonal components of the magnetic field is the ability to determine the course in the full range of pitch, roll and yaw angles that may occur during the flight of a high-maneuver aircraft. The signal from 3D magnetometers can also be used for remote diagnostics of aircraft systems.

The developed algorithms for determining the 3D magnetic deviation were applied e.g. in NSC-1 ORION Helmet Mounted Cueing System designed in the Air Force Institute of Technology. The helmet system is based on magnetic field measurements. Furthermore, in our work, the theoretical basis and metrological aspects of cueing systems were described, as well as were new metrological possibilities resulting from the dynamic development of magnetometers, ADC converters and processors. In pursuing this exploration, our derivations, constructed solutions and gained experiences can be easily transferred to other applications, e.g. control/positioning systems, IPS navigation systems, simulators or virtual reality (VR) systems.

Author Contributions: Conceptualization, JB and AS; data protection, AP; formal analysis, MW; obtaining financing, MW; investigation, AS; methodology, AS; project administration, AS; resources, JB; software, AS; Supervision, AP; validation, JB, MW and AS; visualization, AP and MW; writing - preparing an original project, JB, AP and MW; writing - review and editing, AP and MW. All authors read and agreed to the published version of the manuscript.

Funding: This work was supported by the Ministry of High Education and Science in years 2009-2011 and the National Centre for Research and Development in years 2011-2012 [grant O R00 0063 09] as well as the Ministry of Education and Science and Air Force Institute of Technology in year 2021 [as part of statutory and own research activities].

Institutional Review Board Statement: Not applicable.

Informed Consent Statement: Not applicable.

Data Availability Statement: Sample digital data is available at the Air Force Institute of Technology, Poland.

Acknowledgments:
The authors thank the Ministry of High Education and Science and the National Centre for Research and Development for their support in financing the scientific task enabling the analysis of errors in magnetic field sensors and the development of algorithms for determining spatial deviation in aviation magnetic heading indicating systems.

The authors would like to thank the associates and technical staff of Military Aviation Works No. 2 in Bydgoszcz and air bases in Powidz, Świdwin and Mirosławiec for their help in conducting the research.

Conflicts of Interest: The authors declare no conflict of interest.

REFERENCES

382(X) Magnetic compasses carriage and performance standards, https://puc.overheid.nl/nsi/doc/PUC_2469_14/1/.

AC 43-215 - Standardized Procedures for Performing Aircraft Magnetic Compass Calibration Document Information, FAA 2017, https://www.faa.gov/regulations_policies/advisory_circulars/index.cfm/go/document.information/documentID/1031648.

Accuracy classes of measuring instruments, International Recommendation OIML R34, edition 1979 (E), International Organization of Legal Metrology, https://www.oiml.org/en/files/pdf_r/r034-e79.pdf.

ADIS16405 Triaxial Inertial Sensor with Magnetometer, https://www.analog.com/media/en/technical-documentation/data-sheets/ADIS16405.pdf.

Alken P., Thébault E., Beggan C.D. et al., International Geomagnetic Reference Field: the thirteenth generation. Earth Planets Space 2021, 73, 49, DOI: 10.1186/s40623-020-01288-x.

AMI305 Electronic Compass, ttps://aichi-mi-test.jimdo.com/e-home-new/electronic-compass/ami305-3-axis-compass/.

Bartington Fluxgate Magnetometer, 3-Axis, Low Noise, https://gmw.com/product/mag-03-mag-13/.

Bennett J.S., Vyhnalek B.E., Greenall H., Bridge E.M., Gotardo F., Forstner S., Harris G.I., Miranda F.A., Bowen W.P., Precision Magnetometers for Aerospace Applications: A Review. Sensors 2021, 21, 5568, DOI: 10.3390/s21165568.

Bozorth R.M., Ferromagnetism. Wiley-VCH , August 1993.

Bozorth R.M., The Physical Basis of Ferromagnetism., Bell System Technical Journal, 1 January 1940, 19, pp 1-39, https://archive.org/details/bstj19-1-1/page/n23/mode/2up.

Canciani A., Magnetic Navigation, https://www.gps.gov/governance/advisory/meetings/2018-12/canciani.pdf.

Carletta S., Teofilatto P., Farissi M.S., A Magnetometer-Only Attitude Determination Strategy for Small Satellites: Design of the Algorithm and Hardware-in-the-Loop Testing. Aerospace 2020, 7, 3, DOI: 10.3390/aerospace7010003.

Chulliat A., Brown W., Alken P., Beggan C., Nair M., Cox G., Woods A., Macmillan S., Meyer B., Paniccia M., The US/UK World Magnetic Model for 2020-2025: Technical Report, National Centers for Environmental Information, NOAA, 2020. DOI: 10.25923/ytk1-yx35.

COMSOL Multiphysics® Modeling Software, http://www.comsol.com.

Doerfler R., Magnetic Deviation: Comprehension, Compensation and Computation, 2009, http://www.myreckonings.com/wordpress.

DRV425 Fluxgate Magnetic-Field Sensor, datasheet, Texas Instrument, SBOS729A – October 2015–Revised March 2016.

Ellipse2-A: Miniature AHRS, https://www.navigationsolutions.eu/product/ellipse2-miniature-ahrs/.

EMAG2: Earth Magnetic Anomaly Grid (2-arc-minute resolution), http://geomag.colorado.edu/emag2-earth-magnetic-anomaly-grid-2-arc-minute-resolution.html.

EMAG2: Earth Magnetic Anomaly Grid (2-arc-minute resolution), https://www.ngdc.noaa.gov/geomag/emag2_download.html.

EMWORKS Electromagnetic Simulation Software with Built-in Thermal, Motion and Structural Analyses, https://www.emworks.com.

Enhanced Magnetic Model (EMM), https://www.ngdc.noaa.gov/geomag/EMM/.

Evans P.J. (Owen F.J.), Smith A., Admiralty Manual for the Deviations of the Compass, Hydrographic Office, Admiralty, London 1869, https://archive.org/details/admiralty-manualforthedeviationsoft/mode/1up.

FAA-H-8083-15B Instrument Flying Handbook, U.S. Department of Transportation, Federal Aviation Administration, Flight Standards Service, Oklahoma 2012.

Favor E.R., Anderson T., Design of Helmholtz Coil for Low Frequency Magnetic Field Susceptibility Testing, Naval Undersea Warfare Center, Division Nevport, USA, 1998.

FEMM Finite Element Method Magnetics, https://www.femm.info/wiki/HomePage.

Fescenko I., Jarmola A., Savukov I., Kehayias P., Smits J., Damron J., Ristoff N., Mosavian N., Acosta V.M., Diamond magnetometer enhanced by ferrite flux concentrators, Physical Review Research 2020, 2, 023394, DOI: 10.1103/PhysRevResearch.2.023394.

FXOS8700CQ 6-axis sensor with integrated linear accelerometer and magnetometer, Rev. 8–25 April 2017, https://www.nxp.com/docs/en/data-sheet/FXOS8700CQ.pdf.

Hall Effect Sensing And Application, Honeywell, https://sensing.honeywell.com/hallbook.pdf.

Handbook Of Magnetic Compass Adjustment, National Geospatial-Intelligence Agency, Bethesda, MD 2004.

Haoui A., Kavaler R., Varaiya P., Wireless magnetic sensors for traffic surveillance, Transportation Research Part C: Emerging Technologies, 2008, Vol. 16, Issue 3, 294-306, DOI: 10.1016/j.trc.2007.10.004.

Helmet Mounted Cueing System (HMCS), https://www.thalesdsi.com/our-services/visionix-2/hmcs/.

Helmet mounting systems, Wilcox Industries Corp. 2007, https://patents.justia.com/patent/8826463.

Helmholtz Coils, https://ada.nevis.columbia.edu/~zajc/acad/C1494andC2699/eO-verm/Helmholtz.htm

Hoekstra B., Mhaskar R., MFAM: Miniature Fabricated Atomic Magnetometer for Autonomous Magnetic Surveys, Drones Applied to Geophysical Mapping Workshop SEG 2017, https://seg.org/Portals/0/SEG/News%20and%20Resources/Near%20Surface/Resources/Drones_Workshop/6_MFAM-Miniature%20Atomic%20Magnetometer%20for%20Autonomous%20Magnetic%20Surveys_Hoekstra.pdf.

http://micromagnetics.com.

http://www.dowaytech.com/en/.

http://www.intermagnet.org.

http://www.magnicon.com/fileadmin/download/datasheets/Magnicon_Squids.pdf.

https://aerospace.honeywell.com.

https://intermagnet.github.io/.

https://www.aichi-steel.co.jp/ENGLISH/smart/mi/products/.

https://www.bartington.com/high-precision-magnetometers/.

https://www.bosch-sensortec.com/products/motion-sensors/.

https://www.gemsys.ca.

https://www.geometrics.com.

https://www.nve.com/webstore/catalog/index.php?view=all&cPath=27.

https://www.pnicorp.com.

https://www.sensixs.nl.

https://www.xsens.com/products/.

Inertial Measurement Units (IMU), https://www.analog.com/en/parametricsearch/11172#/.

International Geomagnetic Reference Field, https://www.ngdc.noaa.gov/IAGA/vmod/igrf.html.

ISO 5725-1:1994 Accuracy (trueness and precision) of measurement methods and results – Part 1: General principles and definitions.

ISO 5725-6:1994 Accuracy (trueness and precision) of measurement methods and results – Part 6: Use in practice of accuracy values.

JHMCS II helmet mounted display system, https://jhmcsii.com.

Johnston M.J.S., Review of magnetic and electric field effects near active faults and volcanoes in the U.S.A., Physics of the Earth and Planetary Interiors, 1989, Vol 57, Issue 1-2, 47-63, DOI: 10.1016/0031-9201(89)90213-6.

Joint Helmet Mounted Cueing System (JHMCS), https://elbitsystems.com/product/joint-helmet-mounted-cueing-system-jhmcs/.

 DOI: 10.55676/asi.v4i2.94

Joint Helmet Mounted Cueing System, https://www.boeing.com/history/products/joint-helmet-mounted-cueing-system.page#:~:text=The%20Boeing%20Joint%20Helmet%20Mounted%20Cueing%20System%20%28JHMCS%29,sensors%20and%20weapons%20wherever%20the%20pilot%20is%20looking.

Joint Helmet Mounted Cueing System, https://www.collinsaerospace.com/what-we-do/Military-And-Defense/Displays-And-Controls/Airborne/Helmet-Mounted-Displays/Joint-Helmet-Mounted-Cueing-System

Korepanov V., Marusenkov A., Flux-Gate Magnetometers Design Peculiarities. Surv Geophys 2012, 33, 1059–1079, DOI: 10.1007/s10712-012-9197-8.

Korth H., Strohbehn K., Tejada F., Andreou A.G., Kitching J., Knappe S., Lehtonen S.J., London S.M., Kafel M., Miniature atomic scalar magnetometer for space based on the rubidium isotope 87Rb, J. Geophys. Res. Space Physics, 2016, 121, 7870–7880, DOI: 10.1002/2016JA022389.

Lang F., Blundell S.J., Fourier space derivation of the demagnetization tensor for uniformly magnetized objects of cylindrical symmetry, Journal of Magnetism and Magnetic Materials 2016, 401, 1060-1067, DOI: 10.1016/j.jmmm.2015.10.133.

Lassahn M.P., Trenkler G., Vectorial calibration of 3D magnetic field sensor arrays, in IEEE Transactions on Instrumentation and Measurement, vol. 44, no. 2, pp. 360-362, April 1995, DOI: 10.1109/19.377852.

Liu H., Dong H., Ge, J., Liu Z., An Overview of Technologies for Geophysical Vector Magnetic Survey: A Case Study of the Instrumentation and Future Directions. arXiv 2020, arXiv:2007.05198.

Magnetic Field Sensors, https://www.analog.com/en/parametricsearch/11290#/.

Magnetic Sensors Market - Growth, Trends, Covid-19 Impact, And Forecasts (2021 - 2026), https://mordorintelligence.com/industry-reports/magnetic-sensor-market.

Mohri K., Uchiyama T., Shen L.P., Cai C.M., Panina L.V., Amorphous Wire and CMOS IC-Based Sensitive Micro-Magnetic Sensors (MI Sensor and SI Sensor) for Intelligent Measurements and Controls, Journal of Magnetism and Magnetic Materials, 2002, Vol. 249, No. 1-2, pp. 351-356, DOI: 10.1016/S0304-8853(02)00558-9.

Moskowitz R., Della Torre E., Theoretical aspects of demagnetization tensors, IEEE Transactions on Magnetics, 1966, vol. 2, no. 4, pp. 739-744, DOI: 10.1109/TMAG.1966.1065973.

Notaroš B.M., MATLAB-Based Electromagnetics, Pearson, 2014, 416 pp., https://www.pearson.com/us/higher-education/program/Notaros-MATLAB-Based-Electromagnetics/PGM2486281.html?tab=resources.

OPERA Electromagnetic And Electromechanical Simulation, https://www.3ds.com/products-services/simulia/products/opera/.

Oravec M., Lipovský P., Šmelko M., Adamčík P., Witoś M., Low-Frequency Magnetic Fields in Diagnostics of Low-Speed Electrical and Mechanical Systems. Sustainability 2021, 13, 9197, DOI: 10.3390/su13169197

Ozyagcilar T., Calibrating an eCompass in the Presence of Hard- and Soft-Iron Interference, Freescale Semiconductor Application Note AN4246, https://www.nxp.com/docs/en/application-note/AN4246.pdf.

PalmGauss™ S (PGSC-5G), https://www.aichi-steel.co.jp/ENGLISH/smart/mi/products/palm-gauss.html.

Pazur A., Kowalczyk H., Szelmanowski A., A Study on the Existing Helmet-Mounted Display and Control Systems with Respect to the Optimization of Functions and Applications of a Helmet-Mounted Cueing System, Logistyka 6/2011, 3343-3352, https://docplayer.pl/45371329-Analiza-istniejacych-rozwiazan-systemow-nahelmowego-zobrazowania-i-sterowania-dla-optymalizacji-funkcji-i-sposobu.html.

Pelosi M.J., Patent US7266446B1 Helmet mounted tracking system and method, 2007.

Phillips J.B., Magnetic Navigation, Journal of Theoretical Biology, 1996, Volume 180, Issue 4, Pages 309-319, DOI: 10.1006/jtbi.1996.0105.

Popowski S., Dąbrowski J., The Method of an Error Validation of Integrated Heading Systems, Measurements. Automation. Robotics, 2015, www.researchgate.net/publication/279217602.

Rash C., Helmet Displays in Aviation. Helmet Mounted Display. Design Issues for Rotary-Wing Aircraft, USA, Fort Rucker, 2009.

RM3100 Geomagnetic Sensor, https://www.pnicorp.com/rm3100/.

SC 063 Sight Compass User Instruction Manual, Doc. P/N: 56-101-01200 Revision E, November 7, 2014, Barfield Inc.

Schloss J.M., Barry J.F., Turner M.J., Walsworth R.L., Simultaneous Broadband Vector Magnetometry Using Solid-State Spins, Phys. Rev. Applied 2018, 10, 034044, https://journals.aps.org/prapplied/abstract/10.1103/PhysRevApplied.10.034044.

Singh S.P., Magnetoencephalography: Basic principles. Ann Indian Acad Neurol. 2014;17(Suppl 1):S107-S112. DOI: 10.4103/0972-2327.128676.

Solas Shipborne Navigational Carriage Requirements, https://www.radioholland.com/about-radio-holland/regulations/navigational-carriage-requirements/#150GT.

Space Weather Prediction Center National Oceanic And Atmospheric Administration, https://www.swpc.noaa.gov/.

SQUID Sensors: Fundamentals, Fabrication and Applications, ed. H. Weinstock, NATO ASI Series, Kluwer Academic Publishers 1996, DOI: 10.1007/978-94-011-5674-5.

Szelmanowski A., Borowski J., Cieślik A., Review of Computer-Assist Methods for the Tracking of the Pilot's Helmet Orientation as Applied in the Helmet-Mounted Cueing Systems to Control Military Helicopter's Armament, Logistyka 6/2011, 3633-3640, https://docplayer.pl/158704768-Szelmanowski-andrzej-1-borowski-jerzy-cieslik-andrzej.html.

The World Magnetic Model and Associated Software, https://www.ngdc.noaa.gov/geomag/WMM/soft.shtml.

 DOI: 10.55676/asi.v4i2.94

United States Court of Appeals for the Federal Circuit Elbit Systems Of America, LLC, Appellant v. Thales Visionix, INC., Appellee, 2017-1355, http://www.cafc.uscourts.gov/sites/default/files/opinions-orders/17-1355.Opinion.2-5-2018.1.PDF.

Witos M., Szelmanowski A., Pazur A., Borowski J., Research on errors of magnetic field sensors and algorithms for determining 3D spatial deviation in aeronautical heading reference systems, 2021 IEEE 8th International Workshop on Metrology for AeroSpace (MetroAeroSpace), 23-25 June 2021, pp. 25-30, DOI: 10.1109/MetroAeroSpace51421.2021.9511761.

Witos M., Zaworski T., Mazurek P., Draganová K., Bogucki K., A Passive Magnetic State Observer in Aviation?, Conference: III International Scientific and Technical Conference 'Safety Management in Techniques, Technologies and Transport Policy', 27 29.11.2019, Szczyrk, DOI: 10.13140/RG.2.2.23244.56965.

XEN1210 Magnetic Sensor, datasheet, www.sensixs.nl.

XEN1210 Magnetic Sensor, https://www.sensixs.nl/data/documents/XEN1210.pdf.